

## ORIGINAL PAPER

# The morphology and evolution of chondrichthyan cranial muscles: A digital dissection of the elephantfish *Callorhinchus milii* and the catshark *Scyliorhinus canicula*

Richard P. Dearden<sup>1</sup>  | Rohan Mansuit<sup>1,2</sup>  | Antoine Cuckovic<sup>3</sup> | Anthony Herrel<sup>2</sup>  | Dominique Didier<sup>4</sup> | Paul Tafforeau<sup>5</sup>  | Alan Pradel<sup>1</sup>

<sup>1</sup>CR2P, Centre de Recherche en Paléontologie–Paris, Muséum national d'Histoire naturelle, Sorbonne Université, Centre National de la Recherche Scientifique, Paris cedex 05, France

<sup>2</sup>UMR 7179 (MNHN-CNRS) MECADEV, Département Adaptations du Vivant, Muséum National d'Histoire Naturelle, Paris, France

<sup>3</sup>Université Paris Saclay, Saint-Aubin, France

<sup>4</sup>Department of Biology, Millersville University, Millersville, PA, USA

<sup>5</sup>European Synchrotron Radiation Facility, Grenoble, France

## Correspondence

Richard P. Dearden, CR2P, Centre de Recherche en Paléontologie–Paris, Muséum national d'Histoire naturelle, Sorbonne Université, Centre National de la Recherche Scientifique, CP 38, 57 rue Cuvier, F75231 Paris cedex 05, France. Email: richard.dearden@mnhn.fr

## Funding information

The main work was supported by the Paris Ile-de-France Region—DIM “Matériaux anciens et patrimoniaux”—DIM PHARE project, the ESRF (beamline ID19, proposal ec361) and the H.R. & E. Axelrod Research Chair in paleoichthyology at the AMNH.

## Abstract

The anatomy of sharks, rays, and chimaeras (chondrichthyans) is crucial to understanding the evolution of the cranial system in vertebrates due to their position as the sister group to bony fishes (osteichthyans). Strikingly different arrangements of the head in the two constituent chondrichthyan groups—holocephalans and elasmobranchs—have played a pivotal role in the formation of evolutionary hypotheses targeting major cranial structures such as the jaws and pharynx. However, despite the advent of digital dissections as a means of easily visualizing and sharing the results of anatomical studies in three dimensions, information on the musculoskeletal systems of the chondrichthyan head remains largely limited to traditional accounts, many of which are at least a century old. Here, we use synchrotron tomographic data to carry out a digital dissection of a holocephalan and an elasmobranch widely used as model species: the elephantfish, *Callorhinchus milii*, and the small-spotted catshark, *Scyliorhinus canicula*. We describe and figure the skeletal anatomy of the head, labial, mandibular, hyoid, and branchial cartilages in both taxa as well as the muscles of the head and pharynx. In *Callorhinchus*, we make several new observations regarding the branchial musculature, revealing several previously unreported or ambiguously characterized muscles, likely homologous to their counterparts in the elasmobranch pharynx. We also identify a previously unreported structure linking the pharyngohyal of *Callorhinchus* to the neurocranium. Finally, we review what is known about the evolution of chondrichthyan cranial muscles from their fossil record and discuss the implications for muscle homology and evolution, broadly concluding that the holocephalan pharynx is likely derived from a more elasmobranch-like form which is plesiomorphic for the chondrichthyan crown group. This dataset has great potential as a resource, particularly for researchers using these model species for zoological research, functional morphologists requiring models of musculature and skeletons, as well as for palaeontologists seeking comparative models for extinct taxa.

## KEYWORDS

*Callorhinchus milii*, cranial muscles, digital dissection, elasmobranch, holocephalan, *Scyliorhinus canicula*

## 1 | INTRODUCTION

Cartilaginous fishes (Chondrichthyes) comprise only a small fraction of modern jawed vertebrate diversity (Nelson et al., 2016) but are key to understanding the evolution of jawed vertebrates. As the sister group to the more diverse and disparate osteichthyans (ray-finned fishes, lobe-finned fishes, and tetrapods), their anatomy and physiology provides a valuable outgroup comparison, albeit one which is sometimes incorrectly held to represent jawed vertebrate “primitive states”. The greatly divergent cranial morphologies displayed by the two constituent sister groups of Chondrichthyes—elasmobranchs and holocephalans—have themselves generated much debate, both over chondrichthyan origins and those of jawed vertebrates more broadly. For these reasons, anatomists, embryologists, and physiologists have intensively studied chondrichthyan anatomy over the last two centuries. Recently, tomographic methods have allowed the advent of “digital dissections”, where an organism’s anatomy can be non-destructively visualized and communicated in the form of interactive datasets. These studies have run the gamut of mammals (Cox & Faulkes, 2014; Sharp & Trusler, 2015), archosaurs (Klinkhamer et al., 2017; Lautenschlager et al., 2014), lissamphibians (Porro & Richards, 2017), and actinopterygians (Brocklehurst et al., 2019). Although a few aspects of cartilaginous fish musculoskeletal anatomy have been examined using these methods (Camp et al., 2017; Denton et al., 2018; Tomita et al., 2018), three-dimensional information on the cranial musculoskeletal system is limited.

We address this with a digital dissection of the hard tissues and musculature of two representatives of the Chondrichthyes: *Callorhynchus milii* Bory de Saint-Vincent 1823, a holocephalan, and *Scyliorhinus canicula* Linnaeus 1758, an elasmobranch. *C. milii* is a callorhynchid, the sister group to all other holocephalans (Inoue et al., 2010; Licht et al., 2012), and historically one of the best known holocephalans due to its being one of only two species to inhabit shallow, nearshore waters (Didier, 1995). As a result, the musculature of the genus has been described several times (Edgeworth, 1935; Kesteven, 1933; Luther, 1909a; Ribbink, 1971; Shann, 1919), most recently with Didier (1995) providing a detailed overview of the anatomy and systematics of holocephalans, including *Callorhynchus*. *S. canicula* is a scyliorhinid, a carcharhiniform galeomorph elasmobranch. Because of the accessibility of adults, eggs, and embryos to European researchers (it is abundant in nearshore habitats in the northeastern Atlantic), the species has featured heavily in embryological and physiological studies of chondrichthyans (de Beer, 1931; Coolen et al., 2008; Hughes & Ballintijn, 1965; Oulion et al., 2011; Reif, 1980). While accounts exist of *Scyliorhinus* gross anatomy (Allis, 1917; Edgeworth, 1935; Luther, 1909b; Nakaya, 1975; Ridewood, 1899; Soares & Carvalho, 2013), they are surprisingly rare in comparison to the similarly common *Squalus*, detailed and illustrated accounts of which abound both in the scientific literature (e.g. Marinelli & Strenger, 1959) and the anatomy classroom (e.g. Gilbert, 1965).

Here, we use a synchrotron tomographic dataset to provide accounts of anatomy of the cartilages and musculature of the head in *C. milii* and *S. canicula*. We examine dissection-based reports of muscle anatomy in the light of our reconstructed models. By combining this information with what is known about fossil taxa, we assess scenarios of morphological evolution of chondrichthyan cranial muscles. More broadly, we aim to provide the research community with valuable three-dimensional data on the anatomy of these taxa.

## 2 | METHODS

Both specimens described here are the same as those used in Pradel et al. (2013).

The specimen of *C. milii* is a female at embryonic stage 36 (Didier et al., 1998), the stage immediately prior to hatching, and was originally collected from a spawning site in the Marlborough Sounds, New Zealand, and subsequently stored in 70% ethanol. Animal welfare protocols were followed according to American Society of Ichthyologists and Herpetologists guidelines. All necessary permissions and permits were obtained, and copies are now stored at the Academy of Natural Sciences in Philadelphia (see Pradel et al., 2013). It was scanned in a 75% ethanol solution at a voxel size of 30 microns, and a single propagation distance of 4 m. A U17.6 undulator was used to produce the beam, closed at a gap of 13.5 mm, filtered by 2 mm of aluminium and 1 mm of copper, with an effective energy of 55 keV. A single distance phase retrieval process was used to gain differential contrast of the specimen’s tissues (Pradel et al., 2013). Six subscans of 4 min each were carried out, with 2499 0.1 s projections over 360 degrees. The detector used a 750- $\mu\text{m}$ -thick LuAG scintillator, coupled to a FReLoN CCD camera through a lens-based optic system.

The *S. canicula* specimen is a juvenile, reared at the Laboratoire Evolution, Génome et Spéciation, UPR 9034 CNRS, Gif-Sur-Yvette, France (licensing details given in Pradel et al., 2013), which had reached the stage of independent feeding when humanely killed. It was anaesthetized with MS222 (Sigma) before sacrifice and subsequently fixed with 4% paraformaldehyde and preserved in 100% ethanol solution. It was scanned in a 100% ethanol solution using a holotomographic approach at a voxel size of 7.45 microns. Four propagation distances (20, 150, 400 and 900) were used to retrieve phase maps. A 20 keV monochromatized beam was used, with 1200 0.6 s projections over 180 degrees taken for each propagation distance.

Volumes for both specimens were reconstructed using the ESRF software PyHST. Subvolumes were corrected for ring artefacts, and then concatenated to make a single stack of tif slices. Segmentations of the 3D data were carried out using Mimics versions 15–21 (Materialize). Images of the resulting three-dimensional models were created using Blender v2.80 (blender.org).

The resolution of the scans was not sufficient to observe innervation in most cases, so this is done throughout the text with reference to the literature.

## 3 | RESULTS

The cranial skeletons of *C. milii* and *S. canicula* have been figured and described before (e.g. *Callorhynchus*: Didier, 1995; Finarelli & Coates, 2014; Kesteven, 1933; *Scyliorhinus*: de Beer, 1931; Parker, 1878), but below we provide a brief description of the neurocranial and pharyngeal skeleton to supplement our account of the muscles. We also describe the muscles' attachments and innervation. Where necessary we note disagreements about precise accounts of the innervation of the cranial muscles. All 3D files supporting this research are freely available via morphoMuseum (Dearden et al., 2021) and are included in the supplement as 3D pdfs (*Callorhynchus*, Figure S1; *Scyliorhinus*, Figure S2) and as videos (*Callorhynchus*, Video S1; *Scyliorhinus*, S2).

3.1 | *Callorhynchus milii*

## 3.1.1 | Cranial cartilages

The head skeleton of *Callorhynchus* comprises the neurocranium (Figure 1), to which the palatoquadrates are fused, the mandible formed from the two medially fused Meckel's cartilages, a series of six paired labial cartilages surrounding the mouth, a non-suspensory hyoid arch and five branchial arches (Figure 2). Like all other living holocephalans, the head skeleton is antero-posteriorly compact: the lower jaw extends posteriorly only as far as the back of the orbits, and all other pharyngeal cartilages are located ventral to the neurocranium. The whole arrangement is posteriorly bounded by ventrally joined scapulocoracoids.

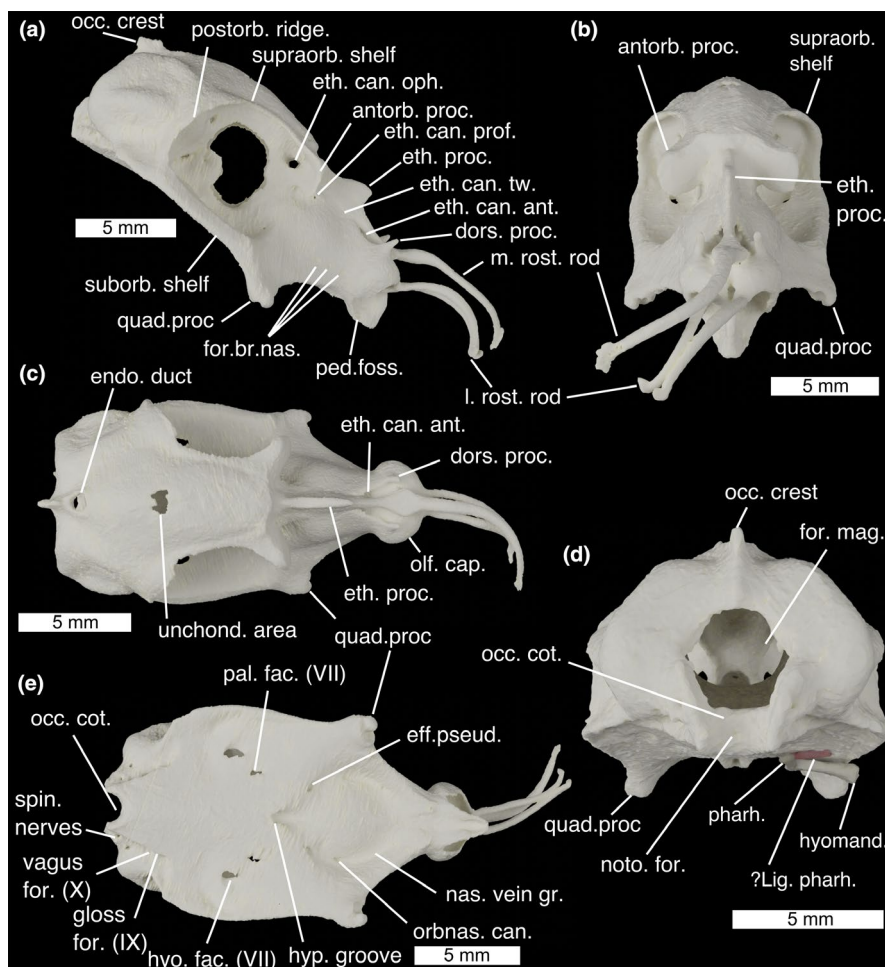


**FIGURE 1** The neurocranium of *Callorhynchus milii* in (a) lateral, (b) anterior, (c) dorsal, (d) posterior and (e) ventral views. ?*lig. pharh.*, ?*ligamentum pharyngohyoideus*; antorb. proc., antorbital process; dors. proc. dorsal process; eff. pseud., foramen for the efferent pseudobranchial artery; endo. duct, foramen for endolymphatic duct; eth. can. Ant, anterior ethmoid canal foramina eth. can. oph, entry into ethmoid canal for superficial ophthalmic complex; eth. can. prof, entry into ethmoid canal for profundus nerve; eth. can. tw., exit from ethmoid canal for twigs of the superficial ophthalmic complex/profundus; eth. proc., ethmoid process; for. br. nas., foramina for branches of the nasal vein; for. mag., foramen magnum; gloss for. (IX), foramen for glossopharyngeal (IX) nerve; hyo. fac. (VII), foramen for hyomandibular branch of the facial (VII) nerve; hyomand., hyomandibula; hyp. groove., hypophyseal groove; l. rost. rod, lateral rostral rod; m. rost. rod, median rostral rod; nas. vein gr., groove for the nasal vein; noto. for., notochord foramen; occ. cot., occipital cotylus; occ. crest, occipital crest; olf. cap., olfactory capsules; orbnas. can., foramen for the orbitonasal canal; pal. fac. (VII), foramen for palatine branch of the facial (VII) nerve; ped. foss., fossa for pedicular cartilage; pharh, pharyngohyal; postorb. ridge, postorbital ridge; quad. proc., quadrate process; spin. nerves, foramina for anterior spinal nerves; suborb. shelf, suborbital shelf; supraorb. shelf, supraorbital shelf; unchond. area, incompletely chondrified area; vagus for. (X), foramen for vagus (X) nerve

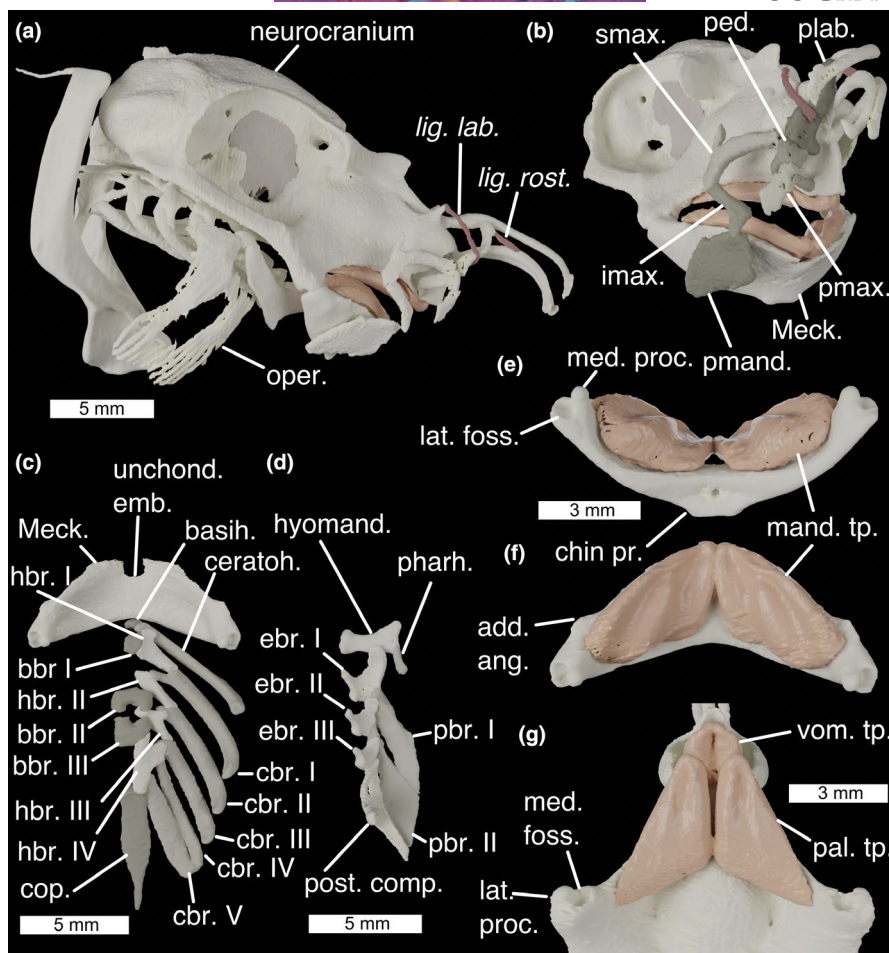


**FIGURE 2** The cranial skeleton of *Callorhynchus milii* (a) complete skeleton in lateral view, (b) antero-lateral view showing labial cartilages, (c) ventral pharyngeal skeleton in dorsal view, (d) dorsal pharyngeal skeleton in ventral view, lower jaw in ventral (e) and dorsal (f) view, and (g) palate in ventral view. Colours: cream, cartilage; beige, sphenoptic membrane; red, ligaments. add. ang., adductor mandibulae angle; basih., basihyal; bbr., basibranchials; cbr., ceratobranchial; ceratoh., ceratohyal; chin pr., chin process; cop., basibranchial copula; ebr., epibranchial; hbr., hypobranchial; hyomand., hyomandibula; imax., inferior maxillary cartilage; lat. foss., lateral fossa of Meckel's cartilage; lat. proc., lateral process of quadrate; lig. lab., ligamentum labialis; lig. rost., ligamentum rostralis; mand. tp., mandibular toothplates; Meck., Meckel's cartilage; med. foss., medial fossa of quadrate; med. proc., medial process of Meckel's cartilage; oper., opercular cartilage; pal. tp., palatine toothplates; pbr., pharyngobranchial; ped., pedicular cartilage; pharh., pharyngohyal; plab., prelabial cartilage; pmand., premandibular cartilage; pmax., premaxillary cartilage; post. comp., posterior epibranchial/pharyngobranchial complex; smax., superior maxillary cartilage; unchond. emb., unchondrified embayment; vom. tp., vomerine toothplates

The **neurocranium** of *C. milii* is tall, with an extensive rostrum, enlarged orbits and a laterally broad otic region (Figure 1). The olfactory capsules (Figure 1c; olf. cap.) take the form of two rounded, ventrally open bulbs, closely set at the extreme anterior end of the neurocranium. A short dorsal process (Figure 1a,c; dors. proc.) projects from the apex of each capsule. Between the olfactory capsules three long rostral rods project anteriorly to support the animal's "trunk": one median rod along the midline (Figure 1a,b; m. rost. rod) and a pair of lateral rods (Figure 1a,b; l. rost. rod). Below them a beak projects ventrally, forming the anterior end of the mouth's roof, and carrying the vomerine toothplates (Figure 2g; vom. tp.). At the very base of the beak's lateral sides are a pair of small fossae with which the pedicular cartilages articulate (Figure 1a, ped. foss.). The ethmoid region is long, with steeply sloping sides separated at the midline by the

ethmoid crest which has a marked ethmoid process at its middle (Figure 1a–c, eth. proc.). A pair of foramina in the orbits form the entrance to the ethmoid canal for the superficial ophthalmic complex (Figure 1a; eth. can. oph.), which runs anteriorly through the midline length of the ethmoid region. About two fifths of the way along the canal's length, it is punctured by a lateral foramen for the entry of the profundus ( $V_1$ ) nerve (Figure 1a; eth. can. prof.), anterior to this several small foramina along its length allow twigs of the superficial ophthalmic complex + profundus to exit onto the ethmoid surface (Figure 1a; eth. can. tw.). The canal opens anteriorly through a pair of teardrop-shaped foramina posterior to the nasal capsules (Figure 1a,c; eth. can. ant.). On the ventral slope of the ethmoid region, a row of three foramina provide passage for branches of the nasal vein behind the nasal capsules (Figure 1a; for. br. nas.). At the postero-ventral corner of the ethmoid region

are a pair of stout quadrate processes (Figure 1a,b,e; quad. proc.), which flare laterally to meet the Meckelian cartilages (Figure 2b; Meck.).

The orbits in *Callorhynchus* are very large, occupying the neurocranium's full height and about two fifths of its length. Anteriorly they are bounded by laterally projecting antorbital processes (Figure 1a,b; antorb. proc.) and a preorbital fascia (Didier, 1995). The inner orbital wall is formed by an extensive sphenoptic membrane (Figures 2 and 3). Posterior to the antorbital processes, the roof of the neurocranium pinches in laterally, meaning that there is only a narrow supraorbital shelf (Figure 1a,b; supraorb. shelf) before the neurocranial roof expands posteriorly into the postorbital ridge (Figure 1a; postorb. ridge), which curves ventrally to form the rear wall of the orbit. Ventrally the orbits are bounded by a broad, flat suborbital shelf (Figure 1a; suborb. shelf), which at its lateral extent broadens into a marked ridge. Just above the level of the suborbital shelf is a large foramen in the sphenoptic membrane for the optic (II) nerve (Figure 3a,b; opt. (II) op.), and immediately posteriorly to this is a small opening for the central retinal (optic) artery (Figure 3a,b; ret. art.). Antero-ventrally there is a small orbitonasal canal foramen for the nasal vein (Figure 3a; orbnas. can.). The superficial ophthalmic complex (V + anterodorsal lateral line) enters the orbit through a dorso-posterior foramen (Figure 3a,b; sup. oph. for.), and then exits, entering the ethmoid canal, via a large ophthalmic foramen in the antero-dorsal part of the orbit (Figure 3a; oph. for.). In the postero-ventral corner of the orbit is a large foramen through which the trigeminal (V) and facial (VII) nerves enter the orbit (Figure 3a,b; for. V+VII). Two foramina in the ventral part of the orbit provide exits for the hyomandibular (Figures 1e and 3b; hyo. fac. (VII)) and palatine (Figures 1e and 3b; pal. fac. (VII)) branches of the facial nerve onto the neurocranial floor. The orbital artery also enters the orbit through the palatine foramen.

Between the orbits, the neurocranial roof forms a shallow convex surface, which becomes more pronounced posteriorly. This

shallow roof curves slightly ventrally, and at its apex is a small, unchondrified area (Figure 1c; unchond. area). The roof pinches in laterally to meet the endolymphatic duct opening (Figure 1c; endo. duct), which is large and subcircular. Posteriorly to this is an occipital crest (Figure 1d; occ. crest), which is pronounced dorsally, before becoming lower and being interrupted by the foramen magnum. The otic capsules form two pronounced bulges on either side of the neurocranium, with the anterior, posterior, and lateral canals forming a rough triangle of ridges, dorso-anteriorly, posteriorly, and laterally. Ventral to the lateral ridge, the sides of the neurocranium pinch in before expanding again to form the edge of the neurocranial floor. The foramen magnum (Figure 1d; for. mag.) is a large circular opening about half the height of the neurocranium, ventral to which is the shallow, rectangular occipital cotylus (Figure 1d; occ. cot.), bounded by two long, thin condyles sit on either side. A small foramen in the centre of the occipital cotylus permits entry for the notochord (Figure 1d; noto. for.), which extends anteriorly into the *dorsum sellae*.

The ventral surface of the neurocranium is markedly broad and flat, tapering and becoming slightly convex anteriorly where it forms the roof of the mouth. The palatine toothplates (Figure 2g; pal. tp.) sit between the vomerine toothplates and the quadrate processes. At the approximate centre of the neurocranial floor lies in a deep hypophyseal groove (Figure 1e; hyp. groove.). Postero-laterally to the hypophyseal groove are the two paired foramina through which the hyomandibular (Figures 1e and 3b; hyo. fac. (VII)) and palatine (Figures 1e and 3b; pal. fac. (VII)) branches of the facial nerve (VII) exit the orbit. Antero-laterally to the hypophyseal groove are a pair of foramina through which the efferent pseudobranchial arteries enter the braincase (Figure 1e; eff. pseud.). Anteriorly to these are paired orbitonasal canals through which the nasal veins pass into the orbit (Figure 1e; orbnas. can.), which mark the posterior end of paired grooves carrying the nasal veins over the neurocranial floor from the nasal capsule to the orbits (Figure 1e; nas. vein gr.).

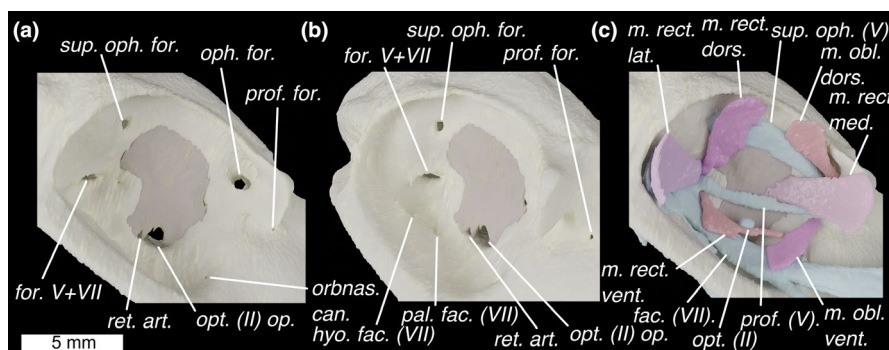


**FIGURE 3** The orbit of *Callorhynchus milii* shown in lateral view with skeleton in (a) lateral and (b) antero-lateral view and (c) lateral view with external optic muscles and cranial nerves. Colours as in Figure 3 with light-blue for cranial nerves. fac. (VII), facial (VII) nerve; for., foramen for superficial ophthalmic complex's entry into orbit; for. V+VII, foramen for entry of trigeminal (V) and facial (VII) nerves into the orbit; hyo. fac. (VII), foramen for hyomandibular branch of the facial (VII) nerve; m. obl. dors., m. obliquus dorsalis; m. obl. vent., m. obliquus ventralis; m. rect. dors., m. rectus dorsalis; m. rect. lat., m. rectus lateralis; m. rect. med., m. rectus medialis; m. rect. vent., m. rectus ventralis; oph. for. ophthalmic foramen; opt. (II) op., optic nerve opening; opt. (II), optic nerve; orbnas. can., foramen for the orbitonasal canal; pal. fac. (VII), foramen for palatine branch of the facial (VII) nerve; prof. (V), profundus (V) nerve; prof. for., foramen for profundus; ret. art., retinal artery opening; sup. oph. (V), superficial ophthalmic complex (V+anterodorsal lateral line nerves); sup. oph

Posteriorly, either side of the neurocranial floor tapers medially and joins the otic region, while the central floor continues posteriorly to form the base of the occiput. Just dorsally to this is a row of foramina for the glossopharyngeal (IX) nerve (Figure 1e; gloss for. (IX)), vagus (X) nerve (Figure 1e; vagus for. (X)) and anterior spinal nerves (Figure 1e; spin. nerves).

**Meckel's cartilages** (Figure 2b; Meck.) are fused at a medial symphysis to form a single, bow-shaped element. This element has a flat surface, the ventral face of which is shallowly convex. Shallow fossae in the dorsal surface carry the mandibular tooth-plates (Figure 2e,f; mand. tp.). The ventro-posterior midline deepens into a pronounced chin process (Figure 2e; chin pr.) onto which the *m. mandibulohyoidei* attach. At the anterior midline is an unchondrified embayment (Figure 2b; unchond. emb.). The articular regions of the mandibular cartilages are positioned at their extreme posterior ends and, as in other chondrichthyans, are double articulating. A lateral process (Figure 2g; lat. proc.) and a medial fossa (Figure 2g; med. foss.) on the quadrate process articulate with a medial process (Figure 2e; med. proc.) and lateral fossa (Figure 2e; lat. foss.) on Meckel's cartilage. Anteriorly to the articulation on each side of the Meckel's cartilage is a small angle over which the *m. adductor mandibulae posterior* attaches (Figure 2f; add. ang.).

Six pairs of **labial cartilages** are present in *Callorhynchus*: the premandibular, inferior maxillary, superior maxillary, pedicular, premaxillary and prelabial. These surround the mouth, supporting the animal's fleshy lip and provide the insertion surfaces for a series of muscles and tendons. The premandibular cartilage (Figure 2b; premand.) is broad and plate-like, sitting laterally to the mandibles. Above it is the short, hockey-stick shaped inferior maxillary (Figure 2b; imax.) cartilage. The dorsal tip of this articulates with the superior maxillary cartilage (Figure 2b; smax.) — a large, curved element with a dorsal process. The anterior tip of this meets the back of the round head of the pedicular cartilage (Figure 2b; ped., which posteriorly curves medially to meet a small fossa in the ethmoid region). Ventrally the head of the pedicular cartilage meets the premaxillary cartilage, a short, flat element which extends into the tissue of the upper lip (Figure 2b; pmax.). Dorsally the head of the pedicular cartilage meets the prelabial cartilage (Figure 2b; plab.), a gentle sigmoid that extends dorsally, and which is secured to the rostral rods by labial and rostral ligaments.

The **hyoid arch** does not articulate with the neurocranium, and comprises a basihyal and paired ceratohyals, hyomandibulae (epihyals) and pharyngohyals. The basihyal (Figure 2c; basih.) is a very small, approximately triangular element with shallow lateral fossae where it articulates tightly with the ceratohyals. The ceratohyal (Figure 2c; ceratoh.) is a large, curved and flattened element, with a pronounced ventral angle. The hyomandibula (Figure 2d; hyomand.), or epihyal, is smaller and flat with sharp angles between each edge forming pronounced, rounded corners. The ventral corner articulates with the ceratohyal, while the dorsal corner articulates with the small, ovoid pharyngohyal (Figure 2d; pharh.). The posterior corner of the hyomandibula is in contact with the opercular cartilage

(Figure 2a; oper.). This has a broad, flat antero-dorsal corner, which divides posteriorly into a series of parallel rays divided roughly into dorsal and ventral zones. Posteriorly to the hyoid arch, no branchial or extrabranchial rays are present.

The **branchial skeleton** comprises five branchial arches, lying entirely ventrally to the neurocranium. The midline floor of the pharynx is formed by a series of basibranchials (Figure 2c; bbr.), a very small anterior one, two middle ones that between them form a box-shape, and a long, posterior basibranchial copula (Figure 2c; cop.). Articulating with these are four paired hypobranchials (Figure 2c; hbr). These are directed antero-medially, each contacting at least two pharyngeal arches. The first hypobranchial contacts the ceratohyal and first ceratobranchial as well as the anterior basibranchial, the second hypobranchial contacts the first and second ceratobranchials, the third hypobranchial contacts the second and third ceratobranchials and extends between the second and third basibranchials, while the fourth hypobranchial is larger than the others and contacts the third, fourth and fifth ceratobranchials in addition to the third basibranchial and the basibranchial copula. The ceratobranchials are gently curved, with short processes to contact the hypobranchials, and the fifth ceratobranchial is slightly flattened and closely associated with the fourth. The first three branchial arches have three separate epibranchials which are flattened and square, with a ventral process that articulates with the ceratobranchials (Figure 2c; cbr). They also have a pronounced anterior process that in the first arch underlies the hyomandibula, and in the posterior arches contacts the anterior pharyngobranchial. Two separate pharyngobranchials (Figure 2d; pbr.) articulate on the posterior corners of the first two epibranchials, projecting posteriorly, also contacting the anterior processes of the second and third epibranchials. They are large and flat, with a dorsal groove over which the second and third efferent branchial arteries pass. At the posterior end of the dorsal branchial skeleton is a complex cartilage (Figure 2d; post. comp.), taking the place of the fourth and fifth epibranchials, as well as the third, fourth and fifth pharyngobranchials. This structure is roughly triangular in shape, and shallowly convex medially, with pronounced postero-ventral and postero-dorsal processes. On its antero-ventral side, it contacts the fourth and fifth ceratobranchials, before projecting anteriorly into a process that contacts the postero-dorsal corner of the third epibranchial. The dorsal surface of this process is obliquely grooved for the fourth efferent branchial artery, and there is a large foramen in this anterior process through which the fifth branchial artery passes.

### 3.1.2 | Cranial musculature

This account follows the terminology of Didier (1995) and Anderson (2008), which itself follows Vetter (1878), Edgeworth (1935) and Shann (1919). For reference regarding muscles' function, Ribbink (1971) gives an account of the functional morphology of the cranial muscles in *Callorhynchus*.



the cartilage medially, separated from it by the *m. intermandibularis* (Figure 4c; *m. intermand.*).

***M. levator anguli oris anterior*** (Figure 4b; *m. lev. ang. oris ant.*)

**Description:** This muscle has an origin on the connective tissue attaching to the antorbital crest. It inserts along the medial side of the anterior part of the superior maxillary cartilage. A bundle of fibres, the *m* (Figure 4b; *m. lev. ang. oris ant. pars. rost.*), extends anteriorly and inserts on the posterior side of the dorsal part of the prelabial cartilage. The fibres of this portion are mixed with those of the *m. levator anguli oris anterior* posteriorly and with those of the *m. labialis anterior* anteriorly.

**Innervation:** Trigeminal (V) nerve (Didier, 1995).

**Remarks:** In male holocephalans, this muscle is functionally linked to the frontal tenaculum (Didier, 1995; Raikow & Swierczewski, 1975). Didier (1995) reported that the *m. levator anguli oris anterior pars rostralis* inserted on the rostral rod in *Callorhinchus*. We find instead that it inserts on the prelabial cartilage, consistent with the states that Didier reports in *Rhinochimaera* and *Chimaera*. Anderson (2008) reports that in *Hydrolagus* fibres of this muscle insert into the mandibular adductor muscles—we can find no evidence for this in *Callorhinchus*.

***M. labialis anterior*** (Figure 4c; *m. lab. ant.*)

**Description:** A small, thin muscle with an origin on the posterior side of the prelabial cartilage, ventrally to the insertion of the *m. levator anguli oris anterior pars rostralis*. It inserts on the dorsal process of and along the dorsal side of the superior maxillary cartilage.

**Innervation:** Trigeminal (V) nerve (Didier, 1995).

**Remarks:** Didier (1995) reports that the origin of this muscle is instead on the anterior tip of the prelabial cartilage. This is plausibly consistent with our data: the resolution of our scans may obscure thin connective tissue wrapping around the cartilage. Either interpretation would presumably give the muscle a different action on the movement of the prelabial cartilage.

***M. intermandibularis*** (Figures 4c and 5b; *m. intermand.*)

**Description:** A thin muscle with an origin along the posterior end and on the dorsal process of the superior maxillary cartilage. It travels ventrally, and has a marked kink posterior to the inferior maxillary

cartilage, corresponding to an internal sheet of tissue separating the muscle into dorsal and ventral parts. It then travels posterior-ventrally where it is interrupted by an insertion on the posterior and medial edges of the premandibular cartilage. It then continues anteriorly to insert on the mandibular symphysis.

**Innervation:** Trigeminal (V) nerve (Didier, 1995).

**Remarks:** This muscle has been variously reported as two separate muscles (Edgeworth, 1902; Kesteven, 1933; Luther, 1909a), or a single muscle interrupted at the premandibular cartilage (Didier, 1995). Here, we follow Didier, who puts forward plausible arguments that both of these parts comprise the same muscle. At the premandibular cartilage, where the two parts meet, there is no clear distinction between them in our scan data.

***M. superficialis*** (Figure 4d; *m. superfic.*)

**Description:** This is a large, very thin muscle, the exact boundaries of which are extremely difficult to make out in the scan data. However, it has a preorbital origin on connective tissue overlying the ethmoid crest. It then travels ventrally to insert along the upper lip, superficially relative to the labial cartilages and all other mandibular muscles, and probably also in the rostrum (Didier, 1995).

**Innervation:** Trigeminal (V) nerve (Didier, 1995).

**Remarks:** Didier (1995) reports that this muscle is unique to *Callorhinchus* among chimaeroids.

***M. constrictor operculi dorsalis*** (Figures 4d and 5b; *m. con. oper. dors.*)

**Description:** A large, superficial muscle forming the opercular flap dorsal to the opercular cartilage. Its origin is at the base of the scapular process, as well as in connective tissue which connects with the notochord (see Didier, 1995) but which is difficult to resolve in our scan data. It inserts on the rim of the operculum, in a mass of connective tissue above the opercular cartilage. The *m. constrictor operculi dorsalis anterior* (Figures 4d and 6c; *m. con. oper. dors. ant.*) is a portion of this muscle with an origin on the ventral rim of the orbit. It extends anteriorly via a tendon which splits to insert on the jaw joint and in the connective tissue of the cheek. The boundary between these two muscles is unresolvable in our scan data.

**Innervation:** Facial (VII) nerve (Didier, 1995).

**Remarks:** The *m. constrictor operculi dorsalis anterior* is only present in *Callorhinchus* among chimaeroids (Didier, 1995).

***M. constrictor operculi ventralis*** (Figures 4d, 5c and 6c; *m. con. oper. vent.*)

**Description:** A large superficial muscle in the ventral part of the opercular flap. Its origin is on the opercular cover, ventrally to the opercular cartilage. It wraps around the bottom of the head to insert ventrally to a fascia that joins it to its antimer. A muscle sheet also travels anteriorly, inserting in the connective tissues of the cheek, overlying the mandible and premandibular cartilage. A mesial sheet derived from the muscle travels dorsally to insert in the connective tissue of the *m. mandibulohyoideus*, posteriorly to Meckel's cartilage.

**Innervation:** Facial (VII) nerve (Didier, 1995).

**Remarks:** Like Didier (1995) we cannot find boundaries between the various component sheets of this muscle described by Kesteven (1933) and consider it to be a single muscle.

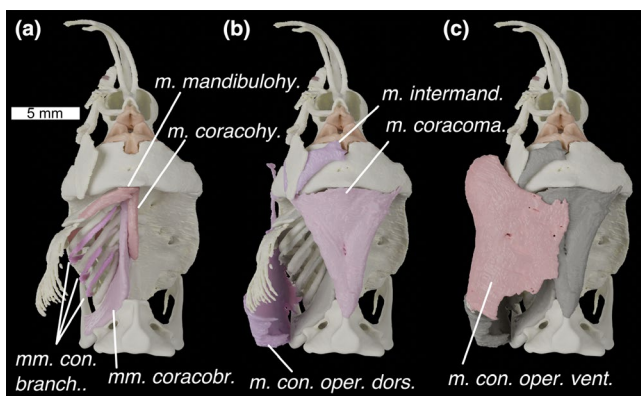


**FIGURE 5** Ventral view of the head of *Callorhinchus milii* with (a) deepest muscles, (b) deeper muscles and (c) shallow muscles overlain. Colours and abbreviations as in Figure 4

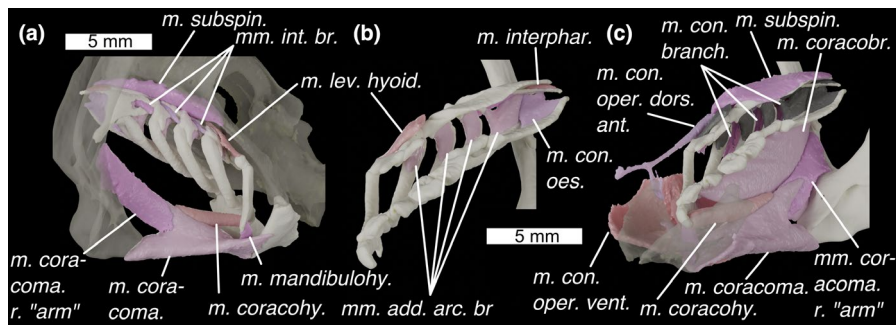


**FIGURE 6** Branchial skeleton of *Callorhynchus milii* with (a) in postero-lateral view with semi-transparent neurocranium and scapulocoracoid, (b) in medial view and (c) in antero-medial view with a semi-transparent mandible. Colours and abbreviations as in Figure 3. Additional abbreviations: *m. con. oes.*, *m. constrictor oesophagi*; *m. coracoma. r. arm*, right “arm” of *m. coracomandibularis* (left not pictured); *m. interphar.*; *m. interpharyngobranchialis*. Otherwise as for Figure 4

***M. levator hyoideus*** (Figures 4a and 6a,b; *m. lev. hyoid.*)

**Description:** This is a small, thin sheet of muscle, with an origin on the underside of the neurocranium, between the foramina for the *nervus hyoideo-mandibularis facialis* and the *nervus palatinus facialis*. It inserts along the ventral part of the epihyal’s postero-lateral edge. It is also linked by connective tissue to the opercular cartilage.

**Innervation:** Facial (VII) nerve (Didier, 1995).

***M. mandibulohyoideus*** (Figures 4a, 5a and 6a; *m. mandibulohy.*)

**Description:** This is a thin muscle with an origin on the posterior symphysis of the mandible, where it meets its antimere as well as the ventral constrictors via a tendon. It inserts on the ventral angle of the ceratohyal.

**Innervation:** The facial (VII) nerve (Didier, 1995) as well as the glossopharyngeal (IX) nerve in *Hydrolagus* (Anderson, 2008).

**Remarks:** Didier (1995) suggests that this muscle is correlated with the evolution of autostyly due to its similarity in position to the mandibular depressor of lungfishes. Kesteven (1933) called this muscle the geniohyoideus, while Didier (1995) called it the interhyoideus. Anderson (2008) coined the name mandibulohyoideus for it, to reflect the muscle’s apomorphy with respect to the interhyoideus and geniohyoideus in osteichthyans, and this is the name we use here.

***Mm constrictores branchiales*** (Figures 4b, 5a and 6c; *mm. con. branch.*)

**Description:** We find three branchial constrictor muscles. These are so small and thin as to be difficult to characterize, but their origins are high up on the lateral sides of epibranchials II and III, and on the lateral side of the posterior pharyngobranchial complex. Each extends antero-posteriorly onto the ventral side of the ceratobranchial of the anterior arch (i.e. ceratobranchials I–III).

**Innervation:** Glossopharyngeal (IX) and vagus (X) nerves (Didier, 1995).

**Remarks:** Like Didier (1995) we were unable to find the fourth branchial constrictor that Edgeworth (1935) described, however, the constrictor muscles are so thin that it is possible that it is unresolved in the scan data. Like Edgeworth (1935) reported, each constrictor passes between two arches. We agree with Didier that the ventral lengths of these muscles are likely described by Kesteven

(1933) as possible *transversi ventrales*: “three long slender muscles, each of which arises from each of the first three basi-branchial cartilages and extends along the outer curve of the ceratobranchial of the same arch”. Kesteven (1933) also describes three sets of “dorsal oblique interarcual muscles”. Of these the “external dorsal oblique muscles” seem likely to be the dorsal part of the branchial constrictors on the basis of descriptions as a “short muscle which arises from the dorsal surface of the epibranchial of the fourth, third, and second arches, and is inserted on the top of the cerato-branchial of the third, second, and third arches”.

***Mm. interarcuales branchiales*** (Figures 4a and 6a; *mm. int. br.*)

**Description:** These muscles are very small and extend from the ventral surface of the pharyngobranchials to the posterior edge of the epibranchials I–III.

**Innervation:** Glossopharyngeal (IX) and vagus (X) nerves (Didier, 1995; Edgeworth, 1935).

**Remarks:** These muscles are not mentioned by Didier (1995) but appear to roughly match the description of the external dorsal oblique muscles by Kesteven (1933), with the difference that they travel from pharyngobranchial to epibranchial rather than from epibranchial to ceratobranchial.

***Mm adductores arcuum branchiales*** (Figures 4a and 6b; *mm. add. arc. br.*)

**Description:** These muscles lie medial to the first four branchial arches, extending between the dorsal surface of the ceratobranchials and the ventral surface of the epibranchials. The origin of the first three is on epibranchials I–III, and they insert on ceratobranchials I–III. The fourth has two origins on the posterior pharyngobranchial complex (pharyngobranchials IV–V) and inserts on ceratobranchials IV–V. Also associated with the fourth is the *m. constrictor oesophagi* (Figure 6b; *m. con. oes.*), the origin of which lies along the posterior process of the posterior-most pharyngobranchial, and which inserts along the postero-lateral length of the basibranchial copula.

**Innervation:** Glossopharyngeal (IX) and vagus (X) nerves (Didier, 1995; Edgeworth, 1935).

**Remarks:** These are probably the lateral internal dorsal oblique muscles of Kesteven (1933), although our data show them to insert

high up on the epibranchial rather than on the pharyngobranchials as described by Kesteven.

**M. cucullaris superficialis** (Figure 4d; *m. cuc. sup.*)

**Description:** A large muscle with a broad origin on the postorbital crest and overlying the epaxial muscles. It inserts on the scapular process, dorsal to the origin of the *m. constrictor operculi dorsalis*.

**Innervation:** Fourth branch of the Vagus (X) nerve (Edgeworth, 1935).

**M. protractor dorsalis pectoralis** (Figure 4b; *m. prot. dors. pect.*)

**Description:** This muscle has its origin on the posterior part of the orbital process and inserts on the anterior edge and medial face of the scapular process. Its boundary with the *m. retractor dorsalis pectoralis* is difficult to distinguish in the scan data.

**Innervation:** Glossopharyngeal (IX) and/or the vagus nerve (X) (Ziermann et al., 2014).

**Remarks:** There is some disagreement over whether this muscle is a trunk muscle or a branchial muscle (see Ziermann et al., 2014), which arises from uncertainty over the innervation.

**M. cucullaris profundus** (Figure 4c; *m. cuc. prof.*) is a short, thin muscle. It has its origin on the underside of the otic region, lateral to the *m. subspinalis*. It inserts on the postero-ventral end of the posterior pharyngobranchial complex's lateral side, latero-ventral to the ceratobranchials.

**Innervation:** Third branch of the vagus (X) nerve (Edgeworth, 1935).

**M. subspinalis** (Figures 4b and 6a,c; *m. subspin.*)

**Description:** Broad and flat with an origin along a stretch of the otic shelf, medial to that of the *m. cucullaris profundus*. It inserts along the dorsal surfaces of pharyngobranchials I and II.

**Innervation:** Spinal nerves, specifically the *plexus cervicalis*, formed by two or more anterior spinal nerves (Edgeworth, 1935).

**M. interpharyngobranchialis** (Figure 6b; *m. interphar.*)

**Description:** This is a very small muscle that joins the second pharyngobranchial to the posterior pharyngobranchial complex.

**Innervation:** Spinal nerves, specifically the *plexus cervicalis*, formed by two or more anterior spinal nerves (Edgeworth, 1935).

**Remarks:** Edgeworth (1935) describes this muscle, while Didier (1995) describes it as absent. It is of such a small size that it might be easily missed.

**M. coracomandibularis** (Figures 4a, 5b and 6a,c; *m. coracoma.*)

**Description:** A very large muscle with its main origin on the T-shaped antero-ventral face of the coracoid region of the pectoral girdle, and which inserts along Meckel's cartilage. Viewed ventrally the muscles are triangular, broadening anteriorly. As described by Shann (1919) and Didier (1995), the muscle is split into shallow and deep portions—the deeper portion inserts along the posterior of the mandible as a sheet, while the shallower portion splits into two thick bundles, which diverge about halfway along the muscles length to insert at either side of Meckel's cartilage. At its anterior extent, the muscle is fairly flat, but towards the origin it develops a pronounced dorsal keel oriented postero-dorsally. This keel is cleft by a v-shaped septum, where the muscle splits into paired “arms” (Figure 6a,c) that diverge laterally to origins on the left and right bases of the scapular processes, dorsal to the pectoral fin articulations.

**Innervation:** Spinal nerves, specifically the *plexus cervicalis*, formed from two or more anterior spinal nerves (Edgeworth, 1935).

**Remarks:** The morphology of this muscle varies in different holcephalan genera (Didier, 1995; Shann, 1919), particularly its relationship to the pectoral symphysis. Both Shann and Didier describe a v-shaped septum in the *m. coracomandibularis* of *Chimaera*, but report that this cannot be found in *Callorhinchus*. Our scan data show it to be present, illustrated in our figures by the junction between the two colours of the muscle. As in Shann's description of *Chimaera*, the spinal nerves that innervate the *m. coracomandibularis* enter the muscle at this septum.

**M. coracohyoideus** (Figures 4a, 5a and 6a,c; *m. coracohy.*)

**Description:** A long thin muscle with its origin on the dorsal surface of the *m. coracomandibularis*, anteriorly to the V-shaped septum. It then extends anteriorly to insert on the posterior side of the basihyal.

**Innervation:** Spinal nerves, specifically the *plexus cervicalis*, formed by two or more anterior spinal nerves (Edgeworth, 1935).

**Remarks:** Didier (1995) notes that it is unclear whether this muscle takes origin from the coracoid or *m. coracomandibularis* in *Callorhinchus*. Our scan data show that its entire origin lies on the *m. coracomandibularis* (Figure 4a).

**Mm. coracobranchiales** (Figures 4b, 5a and 6c; *mm. coracobr.*)

**Description:** Long, thin muscles, with an origin along the dorso-lateral corner of the coracoid and the base of the scapular process. They insert ventrally on the hypobranchials. The anterior three attach to hypobranchials I–III, while the fourth and fifth attach to the fourth, posterior-most, hypobranchial.

**Innervation:** Spinal nerves, specifically the *plexus cervicalis*, formed by two or more anterior spinal nerves (Edgeworth, 1935).

**Remarks:** Although the muscles have separate heads, they are difficult to separate in our scan data and have been segmented out together.

**M. epaxialis** (Figure 4d; *m. epaxialis*).

**Description:** Sheet-like muscle with origin on the top of the head, along the dorsal ridge and above the orbit. It inserts posteriorly with the dorsal myomeres.

**Innervation:** Spinal nerves (Edgeworth, 1935).

**Remarks:** Unlike in *Scyliorhinus* where the epaxials terminate posterior to the orbit, in *Callorhinchus* they extend well anteriorly, terminating in front of the orbits.

**M. retractor dorsalis pectoralis** (Figure 4b; *m. ret. dors. pect.*)

**Description:** This has its origin on the posterior dorsal part of the scapulocoracoid, and along the bottom of the filament which extends posteriorly from the dorsal tip of the scapular process. It extends posteriorly to insert in the trunk musculature.

**Innervation:** Spinal nerves (Didier, 1995).

**M. retractor latero-ventralis pectoralis** (Figure 4b,c; *m. ret. lat-vent. pect. l+m*)

**Description:** This muscle comprises two parts. These have their origin laterally and medially on the scapular process. They insert posteriorly in the dorsal muscle tissue of the body cavity.

**Innervation:** Glossopharyngeal (IX) and/or the vagus nerve (X) (Ziermann et al., 2014).

**Remarks:** There is some disagreement over whether this muscle is a trunk muscle or a branchial muscle (see Ziermann et al., 2014), which arises from uncertainty over the innervation.

**M. retractor mesio-ventralis pectoralis** (Figure 4c; *m. ret. mes.-vent. pect.*)

**Description:** This is a sheet of muscle. Its origin is in several places at the bottom of the scapular process and on the posterior of the coracoid. It inserts in the lateral and ventral muscle of the body.

**Innervation:** Glossopharyngeal (IX) and/or the vagus nerve (X) (Ziermann et al., 2014).

**Remarks:** As above here is some disagreement over whether this muscle is a trunk muscle or a branchial muscle (see Ziermann et al., 2014).

**M. rectus dorsalis** (Figure 3c; *m. rect. dors.*)

**Description:** This is antagonistic to the *m. rectus ventralis*. It has its origin in the orbit anteriorly to the trigeminal nerve entrance. It inserts dorsally around the eye.

**Innervation:** Oculomotor (III) nerve (Edgeworth, 1935).

**M. rectus ventralis** (Figure 3c; *m. rect. vent.*)

**Description:** This muscle is antagonistic to the *m. rectus dorsalis*. It has its origin in the orbit anteriorly to the trigeminal nerve entrance, ventrally the profundus (V) nerve. It inserts ventrally around the eye, with a comparatively broad insertion.

**Innervation:** Oculomotor (III) nerve (Edgeworth, 1935).

**M. rectus lateralis** (Figure 3c; *m. rect. lat.*)

**Description:** This muscle is antagonistic to the *m. rectus medialis*. and has its origin in the orbit anteriorly to the trigeminal nerve entrance. It inserts posteriorly around the eye.

**Innervation:** Abducens (VI) nerve (Edgeworth, 1935).

**M. rectus medialis** (Figure 3c; *m. rect. med.*)

**Description:** This muscle has its origin relatively anteriorly to the other rectus muscles, and is antagonistic to the *m. rectus lateralis*. It inserts anteriorly around the eye.

**Innervation:** Oculomotor (III) nerve (Edgeworth, 1935).

**M. obliquus ventralis** (Figure 3c; *m. obl. vent.*)

**Description:** This muscle is antagonistic to the *m. obliquus dorsalis*. It has its origin just ventral to the antorbital crest, well anteriorly in the orbit. It inserts antero-ventrally around the eye.

**Innervation:** Oculomotor (III) nerve (Edgeworth, 1935).

**M. obliquus dorsalis** (Figure 3c; *m. obl. dors.*)

**Description:** This muscle is antagonistic to the *m. obliquus ventralis*. It has its origin just medial to the antorbital crest, by the ophthalmic foramen. It inserts antero-dorsally around the eye.

**Innervation:** Trochlear (IV) nerve (Edgeworth, 1935).

### 3.1.3 | Ligaments

Didier identifies two paired ligaments in the snout of *Callorhynchus*:

**Ligamentum labialis** (Figure 2a; *lig. lab.*)

**Description:** This travels between a dorsal process on the nasal capsule and then wraps around the antero-ventral part of the prelabial cartilage.

**Remarks:** As Didier (1995) notes this is only present in *Callorhynchus*.

**Ligamentum rostralis** (Figure 2a; *lig. rost.*)

**Description:** This travels between the dorso-anterior part of the prelabial cartilage onto the lateral rostral rod.

**Remarks:** Didier (1995) notes this is only present in *Callorhynchus*.

**?Ligamentum pharyngohyoideus** (Figure 1d; *?lig. pharh.*)

**Description:** A very small ligament (or possibly a slip of muscle) with an origin on the neurocranial floor, posterior to the quadrate processes and lateral to the hypophyseal notch, and inserting on the pharyngohyal dorsally.

**Innervation:** This is presumably innervated by the facial (VII) nerve, given its location, but no precise innervation can be established.

**Remarks:** This structure has not been previously reported. Given that it has not been observed before, and its poor visibility in the dataset, we are cautious its definite existence pending its discovery in gross dissection. However, it is present on both sides of the dataset. Based on the apparent lack of fibres, we presume this is a ligament rather than a muscle, but the latter is certainly not impossible. It may play a role in the operation of the operculum.

## 3.2 | *Scyliorhinus canicula*

### 3.2.1 | Cranial cartilages

The cranial skeleton of *S. canicula* comprises the neurocranium (Figure 7), palatoquadrates, Meckel's cartilages, two pairs of labial cartilages, the hyoid arch and five branchial arches (Figure 8). As in other elasmobranchs, the branchial skeleton stretches well-posterior to the neurocranium, bounded posteriorly by ventrally joined scapulocoracoids.

The **neurocranium** in *Scyliorhinus* is fairly flat, with large orbits and broad ethmoid and otic regions. The olfactory capsules are sub-spherical and very large, taking up about a third of the volume of the entire neurocranium. Ventrally they are open and partially covered by digitate and scrolled projections of cartilage (Figure 7a; *scr. cart.*). They are separated by a medial wall of cartilage which expands ventrally into a narrow internasal plate (Figure 7a; *intn. pl.*). Anteriorly, the olfactory capsules are marked by shallow depressions, in which an anterior grouping of the ampullae of Lorenzini sits (Figure 7d; *ant. Lor.*). This structure is supported by three rostral rods (Figure 7b; *rost. rod m., l.*), one unpaired ventrally and one paired dorsally, which curve, converging centrally. Between the two olfactory cartilages dorsally a large precerebral fontanelle is situated (Figure 7b,d; *pre. font.*).

The orbits are large and oval, comprising about half of the length of the neurocranium. Dorsally they are bounded by a strong supraorbital ridge (Figure 7b; *suporb. ridge*), with sharp anterior and posterior terminations. Posteriorly this forms the

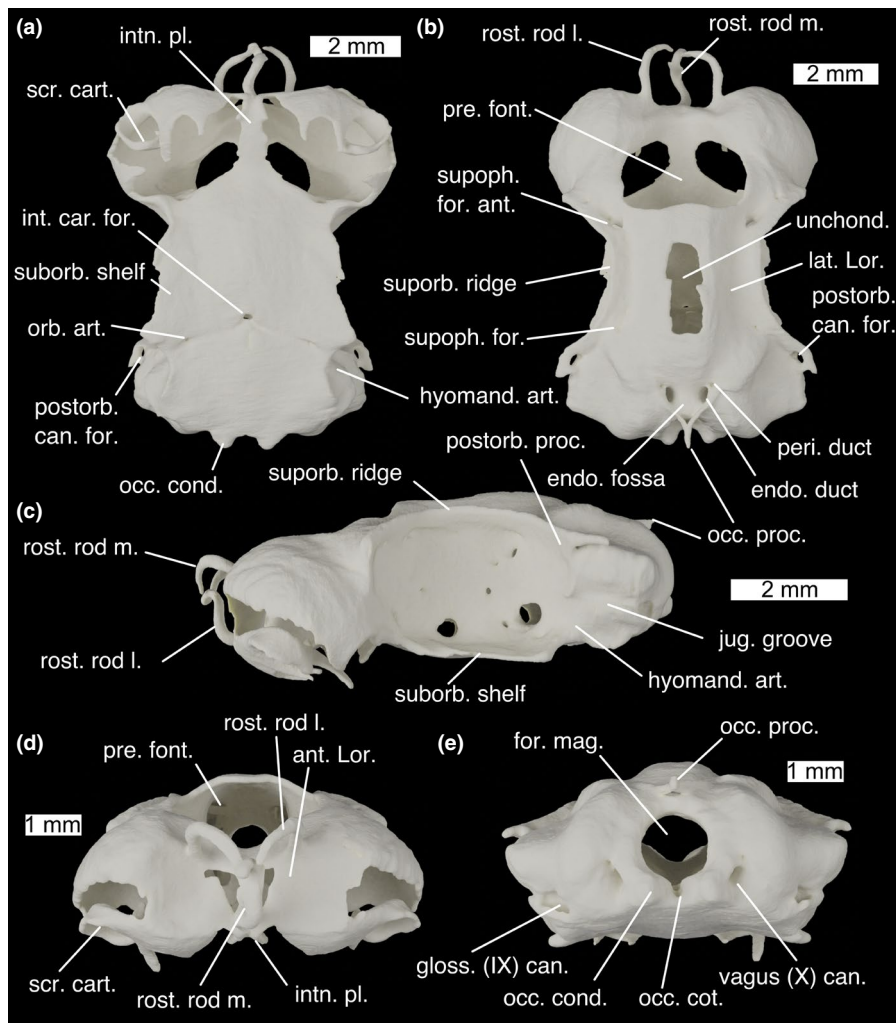


**FIGURE 7** The neurocranium of *Scyliorhinus canicula* in (a) ventral, (b) dorsal, (c) lateral, (d) anterior and (e) posterior views. ant. Lor., anterior depression for ampullae of Lorenzini; endo. duct, endolymphatic duct; endo. fossa, endolymphatic fossa; for. mag., foramen magnum; gloss. (IX) can., glossopharyngeal (IX) nerve canal exit; hyomand. art, hyomandibular articulation surface.; int. car. for., foramen for the internal carotids; intn. pl., internasal plate; jug. groove, jugular groove; lat. Lor., lateral furrows for ampullae of Lorenzini; occ. cond., occipital condyle; occ. cot., occipital cotylus; occ. proc., occipital processes; orb. art., foramen for the orbital artery; peri. duct, perilymphatic duct; postorb. can. for., foramen for postorbital sensory canal; postorb. can. for., foramen for postorbital sensory canal; postorb. proc., postorbital process; pre. font., precerebral fontanelle; rost. rod l, lateral rostral rod; rost. rod m., median rostral rod; scr. cart., scrolled cartilage; suborb. shelf; supoph. for. ant., anterior foramen for the superophthalmic complex; supoph. for. foramina for twigs of the superophthalmic complex; supoph. for., foramina for the superophthalmic complex; suporb. ridge, supraorbital ridge; unchond., incompletely chondrified area; vagus (X) can., vagus (X) nerve canal exit

postorbital process (Figure 7c; postorb. proc.) which, like in other elasmobranchs, does not extend ventrally to form a postorbital arcade. Between the orbits, the roof of the neurocranium rises to form a shallow ridge, the apex of which is incompletely chondrified (Figure 7b; unchond.). Between this and the supraorbital ridges are a pair of shallow furrows carrying ampullae of Lorenzini (Figure 7b; lat. Lor.), which are innervated by twigs of the superficial ophthalmic complex through foramina in the supraorbital ridge (Figure 7b; supoph. for.). The main trunk of the superficial ophthalmic complex enters the orbit through a large foramen postero-dorsally (Figure 9a; supoph. for. post.). A small foramen next to this permits the entry of the profundus into the orbit (Figure 9a; prof. for.). The superficial ophthalmic complex and profundus exit

the orbit together passing through a large foramen in the dorso-anterior corner onto the anterior neurocranial roof (Figures 7b and 9a; supoph. for. ant.). Posterior to this, high up on the wall of the orbit is a small foramen through which the abducens (IV) nerve enters the orbit (Figure 9a; abd. (IV) for.) (Holmgren, 1940). Ventrally the orbit is bounded by a broad suborbital shelf (Figure 7a; suborb. shelf). In the postero-ventral corner of the orbit is a large foramen through which the facial (VII) and trigeminal (V) nerves enter the orbit (Figure 9a; V+VII). Ventro-laterally to this is a small foramen through which the orbital artery enters the orbit (Figure 9a; orb. art.). Antero-dorsally to the facial and trigeminal nerve foramen is an opening for the oculomotor (III) nerve (Figure 9a; oculom. (III) for.) (Holmgren, 1940), while anteriorly to

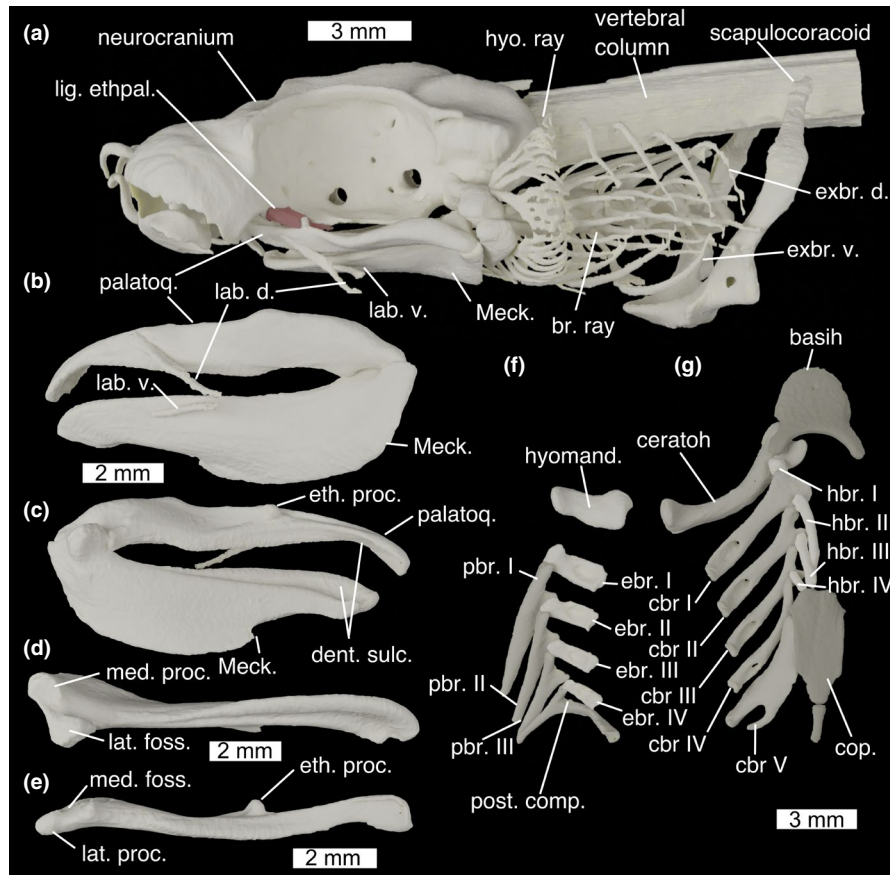


**FIGURE 8** Cranial skeleton of *Scyliorhinus canicula* with (a) whole cranial skeleton in lateral view, mandibles in (b) lateral and (c) medial view, (d) left Meckel's cartilage in dorsal view, (e) left palatoquadrate in ventral view, (f) dorsal gill skeleton in ventral view and (g) ventral gill skeleton in dorsal view. basih., basihyal; br. ray, branchial rays; cbr., ceratobranchial; ceratoh, ceratohyal; cop., basibranchial copula; dent. sulc., dental sulcus; ebr, epibranchial; eth. proc., ethmoid process; exbr. d., dorsal extrabranchial cartilages; exbr. v., ventral extrabranchial cartilages; hbr., hypobranchial; hyo. ray, hyoid rays; hyomand., hyomandibula; lab. d., dorsal labial cartilage; lab. v., ventral labial cartilage; lat. foss., lateral fossa of Meckel's cartilage; lat. proc., lateral process of palatoquadrate; Meck., Meckel's cartilage; med. proc., medial process of Meckel's cartilage; palatoq., palatoquadrate; pbr., pharyngobranchial; post. comp., posterior epibranchial/pharyngobranchial complex

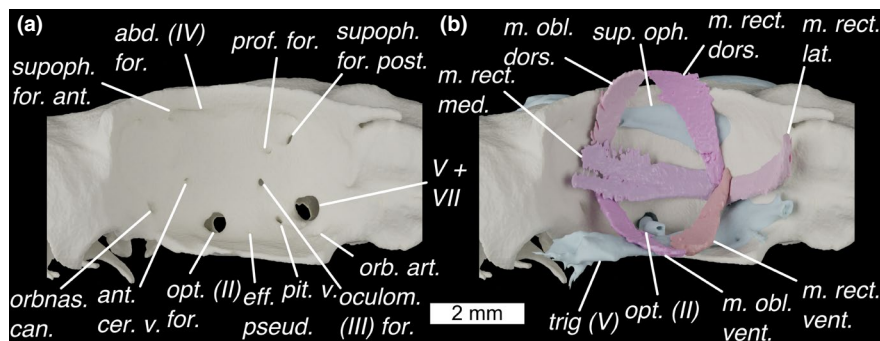


**FIGURE 9** The orbit of *Scyliorhinus canicula* shown in lateral view with (a) foramina shown, and (b) external optic muscles and cranial nerves. Colours as in Figure 9 with light-blue for cranial nerves. abd. (IV) for., foramen for the abducens (IV) nerve; ant. cer. v., foramen for the anterior cerebral vein; eff. pseud., foramen for the efferent pseudobranchial artery; m. obl. dors., m. obliquus dorsalis; m. obl. vent., m. obliquus ventralis; m. rect. dors., m. rectus dorsalis; m. rect. lat., m. rectus lateralis; m. rect. med., m. rectus medialis; m. rect. vent., m. rectus ventralis; oculom. (III) for., foramen for the oculomotor (III) nerve; opt. (II), optic nerve; opt. (II) for., foramen for the optic (II) nerve; orb. art., foramen for the orbital artery; orb. art. ant., foramen for the orbitonasal canal; pit. v., foramen for pituitary vein; prof. for., foramen for profundus; sup. oph., superficial ophthalmic complex (V); supoph. for. ant., anterior foramen for the superophthalmic complex; supoph. for. post., posterior foramen for the superophthalmic complex; trig. (V), trigeminal nerve; V+VII, foramen for entry of trigeminal (V) and facial (VII) nerves into the orbit

it is a foramen for the pituitary vein (Figure 9a; pit. v.) (Holmgren, 1940). Anteriorly to this is a foramen for the efferent pseudobranchial artery (Figure 9a; eff. pseud.), and anteriorly to this the foramen for the optic (II) nerve (Figure 9a; opt. (II) for.) as well as the optic artery. A small foramen antero-dorsal to the foramen for the optic nerve permits entry for the anterior cerebral vein (Figure 9a; ant. cer. v.). A foramen in the antero-ventral corner of the orbit provides an entry for the nasal vein through the orbitonasal canal (Figure 9a; orbnas. can.). Posteriorly to the orbit on the skull roof is a large foramen, through which the postorbital sensory canal passes (Figure 7a; post. can. for.).

The otic capsules are broad and marked by a dorsal ridge formed by the anterior and posterior semicircular canals, with the external semicircular canal forming a pronounced lateral ridge. Below the lateral ridge is a marked groove for the jugular vein (Figure 7c; jug. groove). Antero-ventrally to this lies a flat surface on which the hyomandibula articulates (Figure 7c; hyomand. art.). Posteriorly to this jugular groove is the exit point of the glossopharyngeal (IX) nerve canal (Figure 7e; gloss. (IX) can.). Between the dorsal ridges is a shallow endolymphatic fossa (Figure 7b; endo. fossa), containing paired openings—a larger pair for the endolymphatic ducts (Figure 7b; endo. duct) and a smaller pair antero-laterally for the perilymphatic ducts (Figure 7b; peri. duct). Posteriorly to these are paired occipital processes that join to form an arc (Figure 7b,c; occ. proc.). A rounded foramen magnum (Figure 7e; for. mag.) is positioned below this, and ventrally to this is a shallow occipital cotylus (Figure 7e; occ. cot.), bounded laterally by rounded occipital condyles (Figure 7e; occ. cond.). Laterally to these are a pair of foramina for the exit of the Vagus (X) nerve canal (Figure 7e; vagus (X) can.). At least one of the spinal nerves appears to join the Vagus to leave through the vagal canal: the rest diverge posteriorly to the braincase.

The ventral side of the neurocranium is flat, broad and fairly featureless. At about one third of the length from the posterior, it is punctured by a medial foramen through which the internal carotids enter the neurocranium (Figure 7a; int. car. for.), and lateral to this are paired foramina through which the orbital arteries enter the orbits (Figure 7a; orb. art.).

*Scyliorhinus* also possesses a small prespiracular cartilage, in the anterior wall of the spiracle (Ridewood, 1896; Tomita et al., 2018). However, resolution surrounding the spiracle in our dataset proved insufficient to locate this.

The **palatoquadrates** (Figure 8a,b; palatoq.) are about one third of the length of the neurocranium and joined at an anterior symphysis. They are low and flat, with a short, rounded ethmoid process on the medial face of the palatine process, via which the neurocranium is joined to the palatoquadrate by the ethmopalatine ligament (see below) (Figure 8e; eth. proc.). Anteriorly to this process the dorsal edge is marked by a shallow groove. The inside edge carries a shallow sulcus for the teeth (Figure 8c; dent. sulc.). **Meckel's cartilages** are about one and a half times as deep as the palatoquadrates (Figure 8a,b; Meck.), and are joined at an anterior symphysis. Dorsally it is grooved by a sulcus for the attachment of

teeth (Figure 8c; dent. sulc.). It is ventrally tall, particularly along its posterior half before abruptly losing height. A dorsal and a ventral pair of labial cartilages are positioned lateral to the jaws, which together form a v-shape with the open end anteriorly (Figure 8a,b; lab. d., lab. v.). The elements have a double articulation. A large medial process (Figure 8d; med. proc.) and lateral fossa (Figure 8d; lat. foss.) on Meckel's cartilage articulate with a narrow lateral process (Figure 8e; lat. proc.) and shallow medial fossa (Figure 8e; med. foss.) on the palatoquadrate.

The hyoid arch comprises a basihyal, and paired ceratohyals and hyomandibulae (epihyals). The basihyal is broad and flat (Figure 8f; basihy.), and is punctured centrally by a single foramen for the thyroid gland stalk (De Beer & Moy-Thomas, 1935). A rim curves around its anterolateral edge, and terminates posteriorly, forming paired ceratohyal articulations along with posteriorly projecting paired processes. The ceratohyal (Figure 8f; ceratoh.) is laterally flattened and curved dorsally. The anterior end is expanded into two heads, the anterior of which articulates in the basihyal's fossa. The hyomandibula (Figure 8f; hyomand.) is short and stout, with expanded ends for the articulation with the braincase and the ceratohyal. It articulates on the ventral side of the otic capsule, immediately posterior to the orbit. Hyoid rays (Figure 8f; hyo. ray) are attached to the posterior side of the hyomandibula and ceratohyal, and form a branching series of rays that support the first gill flap.

Posterior to the hyoid arch are five branchial arches. The floor of the pharynx is supported by a basibranchial copula and four hypobranchials. The basibranchial copula (Figure 8f; cop.) is a large, flat, posteriorly located element with a posterior tail, the posterior length of which is mineralized. The anterior-most hypobranchial (Figure 8f; hbr.) is small and cuboid, and oriented anteriorly, overlying the ceratohyal and joining the posterior process of the basihyal to the first ceratobranchial. The posterior three hypobranchials are long and thin, each smaller than the one before, and are oriented posteriorly towards the anterior edge of the copula from the junction between the first and second, second and third, and third and fourth ceratobranchials. The first four ceratobranchials (Figure 8f; cbr.) are long and thin, and their distal end is expanded into two heads, each of which meets the hypobranchial and ceratobranchial of the arches in front and behind. The dorsal proximal surface is marked by a deep spoon-shaped concavity in which the branchial adductor muscles sit, and which is pierced by a foramen, possibly to allow vascularization or innervation of the adductor muscles. The posterior-most ceratobranchial is broad and flat, lacks a distal head and has its proximal end branched into two parts. The first four epibranchials (Figure 8f; ebr.) are short and rectangular with a short anterior process, and concave ventrally for the branchial adductors. They are pierced by a foramen, again possibly for the vascularization or innervation of the branchial adductors. There are three separate pharyngobranchials (Figure 8f; pbr.), which are long, thin arrowheads swept posteriorly. Their proximal ends are expanded into two heads, the anterior one of which articulates with the anterior epibranchial and the posterior one of which overlies the epibranchial behind. The posterior-most

pharyngobranchial(s) and the fifth epibranchial are fused into a single pick-shaped posterior complex (Figure 8f; post. comp.) with an anterior process articulating with the fourth epibranchial, a ventral process articulating with the fifth ceratobranchial and a posterior swept back process. The branchial rays (Figure 8a; br. ray) are unbranched, unlike those of the hyoid, and attached to the ceratobranchials and epibranchials of the first four branchial arches, becoming less numerous on posterior arches. Five dorsal extrabranchial cartilages (Figure 8a; exbr. d.) overlie each gill flap, with heads on the lateral face of the expaxial (I) and cucullaris (II–V) muscle. There are three ventral extrabranchial cartilages (Figure 8a; exbr. v.), supporting the second, third and fourth gill flaps ventrally. These have complex-shaped heads that are ventrally inserted between the coracobranchial muscles and overlying the coracoarcual muscles.

### 3.2.2 | Cranial muscles

This account follows the terminology of Edgeworth (1935). For reference regarding muscles' function, Hughes and Ballintijn (1965) investigate functional morphology of the branchial musculature in *Scyliorhinus*, while feeding mechanics of sharks generally are reviewed by Motta and Huber (2012).

#### *M. levator labii superioris* (Figure 10a; *m. lev. lab. sup.*)

**Description:** A long thin muscle with its origin on the posterior part of the nasal capsule, immediately antero-lateral to the orbit. It extends postero-ventrally to insert in the fibres of the dorsal part of the adductor muscle. It is separated from the *M. adductor mandibulae* by the trigeminal (V) nerve, which lies across the lateral surface, but the border between the fibres of the two muscles are largely indistinguishable in our scan data and are segmented as one model. Fibres of the *m. levator labii superioris* reach the level of the fascia separating the dorsal and ventral parts of the mandibular adductor.

**Innervation:** Trigeminal (V) nerve (Edgeworth, 1935).

**Remarks:** This muscle is variable in galeomorph sharks, with phylogenetic significance (see discussion in Soares & Carvalho, 2013).

#### *M. adductor mandibulae* (Figures 10a and 11a; *m. add. mand.*)

**Description:** This muscle is divided into two parts, dorsal and ventral, and is separated from the *M. levator labii superioris* by the trigeminal (V) nerve. Dorsal and ventral parts are separated by an internal fascia, latero-ventral to the mandibular joint, on which they both insert. The origin of the dorsal part occupies a shallow fossa in the posterior third of the palatoquadrate's lateral face. The origin of the ventral part occupies a shallow fossa in the posterior half of the lateral face of Meckel's cartilage.

**Innervation:** Trigeminal (V) nerve (Edgeworth, 1935).

#### *M. intermandibularis* (Figures 10c, 11c and 12c; *m. intermand.*)

**Description:** This is a broad, flat, triangular muscle with its origin along the posterior margin of the Meckelian cartilages. It then extends posteriorly as a sheet, inserting medio-ventrally on the aponeurosis of the *m. constrictor hyoideus*.

**Innervation:** Trigeminal (V) nerve (Edgeworth, 1935).

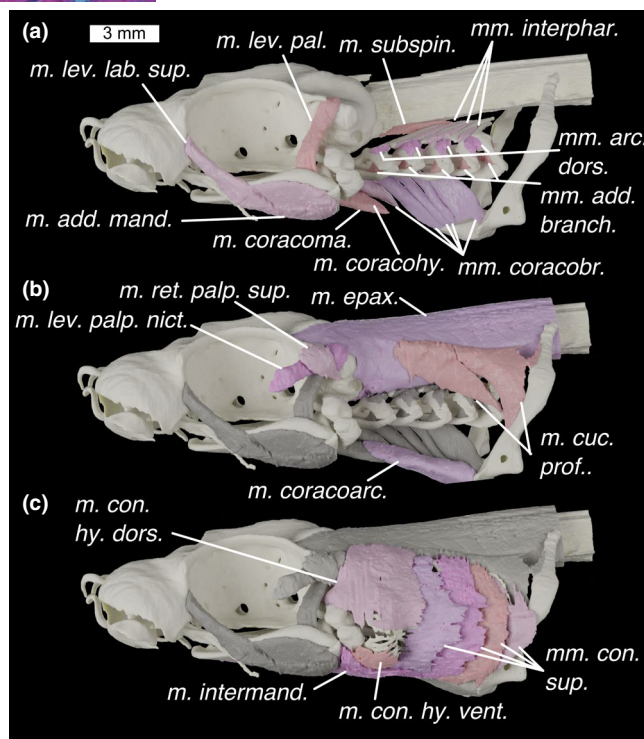


**FIGURE 10** Lateral view of the head of *Scyliorhinus canicula* (a–c) showing progressively more shallow muscles with previous layer/s of muscles shown in grey. Colours: cream, cartilage; beige, pinks, muscles; greys, deeper muscles. *m. add. mand.*, *m. adductor mandibulae*; *m. con. hy. dors.*, *m. constrictor hyoideus dorsalis*; *m. con. hy. vent.*, *m. constrictor hyoideus ventralis*; *m. coracoarc.*, *m. coracoarcualis*; *m. coracohy.*, *m. coracohyoideus*; *m. coracoma.*, *m. coracomandibularis*; *m. cuc. prof.*, *m. cucullaris profundus*; *m. epax.*, *m. epaxialis*; *m. intermand.*, *m. intermandibularis*; *m. lev. lab. sup.*, *m. levator labii superioris*; *m. lev. pal.*, *m. levator palatoquadrate*; *m. lev. palp. nict.*, *m. levator palpebrae nictitantis*; *m. ret. palp. sup.*, *m. retractor palpebrae superioris*; *m. subspin.*, *m. subspinalis*; *mm. add. branch.*, *m. adductors branchiales*; *mm. arc. dors.*, *mm. arcuales branchiales*; *mm. con. sup.*, *mm. constrictors superficiales*; *mm. coracobr.*, *mm. coracobranchiales*; *mm. interphar.*, *mm. interpharyngobranchiales*

**Remarks:** The exact point of insertion is difficult to see in our scan data because it is so thin, but it matches accounts of the same muscle in other elasmobranchs (Soares & Carvalho, 2013; Ziermann et al., 2014).

#### *M. levator palatoquadrate* (Figure 10a; *m. lev. pal.*)

**Description:** A thin muscle with an origin on the latero-ventral side of the otic process, immediately posterior to the postorbital process and ventral to the neurocranial roof. It inserts on the medial side of the palatoquadrate, just anteriorly to the jaw joint, in a shallow depression.

**Innervation:** Trigeminal (V) nerve (Edgeworth, 1935).

#### *M. levator palpebrae nictitantis* (Figure 10b; *m. lev. palp. nict.*)

**Description:** A thin muscle, overlying the *m. levator palatoquadrate*. It has its origin on the dorso-lateral corner of the otic process, dorso-posteriorly to the origin of the *m. levator palatoquadrate* and extends antero-ventrally to insert on the lower eyelid.

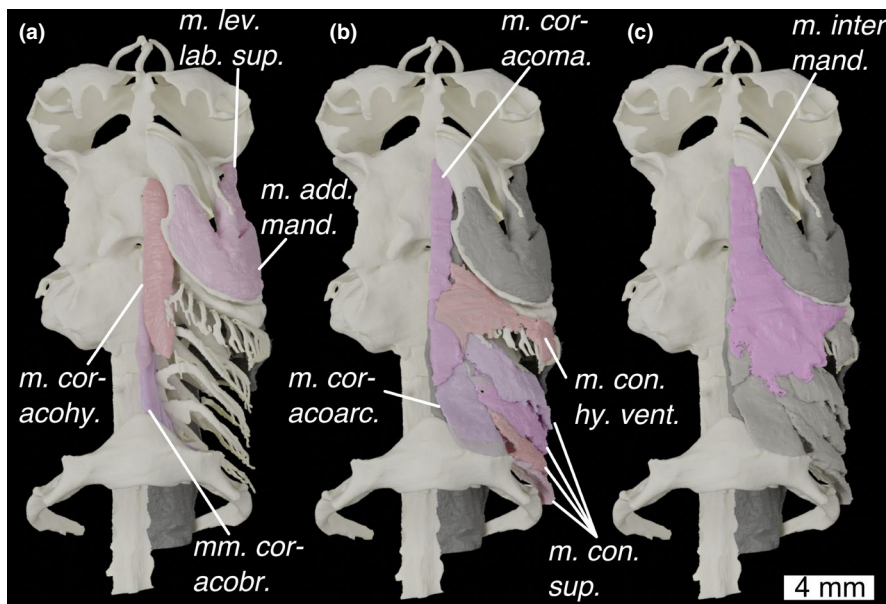


**FIGURE 11** Ventral view of the head of *Scyliorhinus canicula* with (a) deepest muscles, (b) deeper muscles and (c) shallow muscles overlain. Colours and abbreviations as in Figure 10

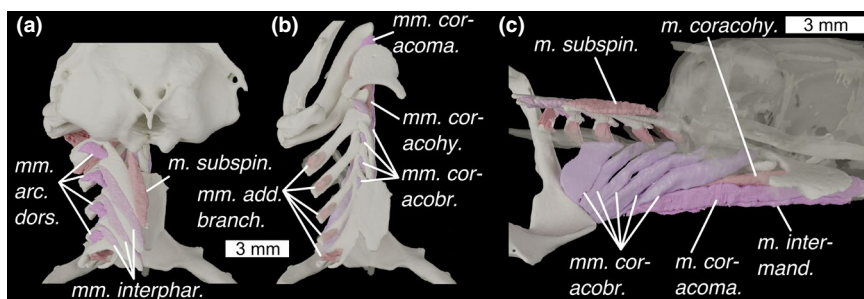


**FIGURE 12** Branchial skeleton of *Scyliorhinus canicula* (a) in dorsal view, with neurocranium (b) in dorsal view with neurocranium removed and dorsal branchial skeleton semi-transparent, and (c) in medial view with neurocranium and central gill-skeleton semi-transparent. Colours and abbreviations as in Figure 10

**Innervation:** Trigeminal (V) nerve (Edgeworth, 1935).

***M. retractor palpebrae superioris*** (Figure 10b; *m. ret. palp. sup.*)

**Description:** This is a short, fat muscle overlying the *m. levator palpebrae nictitantis*. It has its origin on the otic region, ventral to the origin of the *m. levator palpebrae nictitantis*. It travels dorso-anteriorly, overlying the *m. levator palpebrae nictitantis* and inserting on the upper eyelid.

**Innervation:** Trigeminal (V) nerve (Edgeworth, 1935).

**Remarks:** This matches the accounts of Ridewood (1899) and Edgeworth (1935) and are unlike data in Soares and Carvalho (2013), who imply that *Scyliorhinus* has both a *m. retractor palpebrae superioris* and a *m. depressor palpebrae superioris*.

***M. constrictor hyoideus dorsalis*** (Figure 10c; *m. con. hy. dors.*)

**Description:** This is a large thin muscle with a broad origin extending from over the anterior-most *m. constrictor superficiales* and anteriorly over the lateral side of the *m. epaxialis*. The muscle overlies the eyelid muscles and has a further origin on the lateral wall of the otic capsule. The anterior part of the muscle inserts along the

postero-ventral two thirds of the hyomandibula, while posteriorly it overlies the hyoid rays, inserting in the dorsal fibres of the *m. constrictor hyoideus ventralis*.

**Innervation:** Facial (VII) nerve (Edgeworth, 1935).

**Remarks:** This muscle includes the *m. levator hyomandibulae* (the anterior fibres), which are inseparably joined (Soares & Carvalho, 2013). Exact boundaries were difficult to segment out due to the muscle's small width.

***M. constrictor hyoideus ventralis*** (Figures 10c and 11b; *m. con. hy. vent.*)

**Description:** This is a thin, flat muscle with a ventral origin along the medial aponeurosis, underlying the *m. coracomandibularis*. It overlies the hyoid rays and inserts into the fibres of the *m. constrictor hyoideus dorsalis*.

**Innervation:** Facial (VII) nerve (Edgeworth, 1935).

**Remarks:** Exact boundaries were difficult to segment out due to the muscle's small width.

***M. constrictor spiracularis*** (not figured).

**Remarks:** The *m. constrictor spiracularis* lies posterior to the spiracle in *Scyliorhinus* (Ridewood, 1899). However, the contrast surrounding the spiracle was insufficient to resolve this in our scan data.

**M. adductores branchiales** (Figures 10a and 12b; *m. add. branch.*)

**Description:** These are small muscles of which there are five. They have their origin on spoon-shaped fossae on the dorsal surface of each ceratobranchial and insert in shallow fossae in the ventral surface of each corresponding epibranchial. The fifth inserts on the posterior pharyngobranchial complex.

**Innervation:** Vagus (X) and glossopharyngeal (IX) nerves (Edgeworth, 1935).

**Remarks:** Unlike the *Callorhynchus* there is one muscle per branchial arch.

**Mm. arcuales dorsales** (Figures 10a and 12a; *m. arc. dors.*)

**Description:** There are four of these muscles. They have their origin on the lateral surfaces of epibranchials I-IV, and insert on the ventro-lateral edge of each pharyngobranchial, between their anterior and lateral processes.

**Innervation:** Vagus (X) and glossopharyngeal (IX) nerves (Edgeworth, 1935).

**Remarks:** Allis (1917) refers to these as the *mm. arcuales*. We have used Edgeworth's name for clarity.

**Mm. constrictor superficiales** (Figures 10c, 11b and 12c; *mm. con. sup.*)

**Description:** These are very thin sheet-like muscles. They have their origin medially to the *m. cucullaris profundus*, where they insert between the dorsal extrabranchial cartilages. They travel ventrally to the gill bars, and insert ventrally into the medial aponeurosis.

**Innervation:** Vagus (X) and glossopharyngeal (IX) nerves (Edgeworth, 1935).

**M. subspinalis** (Figures 10a and 12a,c; *m. subspin.*)

**Description:** A thin flat muscle with an origin on the postero-ventral edge of the neurocranium, ventral to the occipital condyle, as well as on the ventral side of the spinal column. It then passes posteriorly and inserts on the medial tip of pharyngobranchial I.

**Innervation:** Spinal nerves, specifically the *plexus cervicalis*, formed from two or more anterior spinal nerves (Edgeworth, 1935).

**Mm. interpharyngobranchiales** (Figures 10a and 12a; *Mm. interphar.*)

**Description:** These pass between the pharyngobranchials and are three in number.

**Innervation:** Spinal nerves, specifically the *plexus cervicalis*, formed from two or more anterior spinal nerves (Edgeworth, 1935).

**M. coracomandibularis** (Figures 10a, 11b and 12b,c; *m. coracoma.*)

**Description:** This is a long thin muscle. It has its origin on the posterior part of Meckel's cartilage, and runs posteriorly to insert with the *m. coracohyoideus* and *m. coracobranchiales* muscles ventrally (on the aponeurosis of the *m. constrictor hyoideus centralis*).

**Innervation:** Spinal nerves, specifically the *plexus cervicalis*, formed from two or more anterior spinal nerves (Edgeworth, 1935).

**M. coracohyoideus** (Figures 10a, 11a and 12b,c; *mm. coracohy.*)

**Description:** This is a long thin muscle. It has its origin on the ventral surface of the basihyal, and extends postero-ventrally to attach ventrally (on the aponeurosis of the *m. constrictor hyoideus centralis*).

**Innervation:** This is innervated by spinal nerves, specifically the *plexus cervicalis*, formed by two or more anterior spinal nerves (Edgeworth, 1935).

**Remarks:** Edgeworth calls this the *rectus cervicis* but for consistency we have kept it as *m. coracohyoideus*.

**Mm coracobranchiales** (Figures 10a, 11a and 12b,c; *mm. coracobr.*)

**Description:** These are five in number. The first has its origin anterior to the first ceratobranchial's ventral tip. This pattern continues posteriorly with the II-IV. The Vth one has its origin on ceratobranchial V and the copula. Number I inserts at the medial part with the coracohyoid and mandibular. II-V insert on the coracoid process of the scapular coracoid.

**Innervation:** Spinal nerves, specifically the *plexus cervicalis*, formed from two or more anterior spinal nerves (Edgeworth, 1935).

**M. cucullaris profundus** (Figure 10b; *m. cuc. prof.*)

**Description:** This is a large triangular muscle divided into two parts by an internal septum. The anterior part has its origin in the anterior musculature, between the hyoid constrictor and the epaxial muscles. It inserts on the posterior-most epibranchial. The posterior part inserts along the length of the scapular process.

**Innervation:** Vagus (X) nerve (Edgeworth, 1935).

**M. coracoarcualis** (Figures 10b and 11b, *m. coracoarc.*)

**Description:** A short broad muscle with an origin on the anterior face of the ventral symphysis of the shoulder girdle. It inserts on the ventral aponeurosis, between the *m. coracohyoideus* and the *m. coracobranchiales*.

**Innervation:** Spinal nerves (Edgeworth, 1935).

**M. epaxialis** (Figure 10b; *m. epax.*)

**Description:** Segmented muscles with an origin on the posterior part of the dorsal surface of the neurocranium, in broad fossae over the otic capsule. It inserts posteriorly with the dorsal myomeres.

**Innervation:** Spinal nerves (Edgeworth, 1935).

**M. rectus dorsalis** (Figure 9b; *m. rect. dors.*)

**Description:** This is antagonistic to the *m. rectus ventralis*. It has its origin in the posterior part of the orbit, antero-dorsally to the foramen for the V+VII nerves and below the entry for the superficial ophthalmic complex. It inserts dorsally over the eye.

**Innervation:** Oculomotor (III) nerve (Edgeworth, 1935).

**M. rectus ventralis** (Figure 9b; *m. rect. vent.*)

**Description:** This is antagonistic to the *m. rectus dorsalis*. It has its origin immediately posterior to the former's origin, above the foramen for the V+VII nerves. It inserts ventrally around the eye.

**Innervation:** Oculomotor (III) nerve (Edgeworth, 1935).

**M. rectus lateralis** (Figure 9b; *m. rect. lat.*)

**Description:** This is antagonistic to the *m. rectus medialis*. It has its origin in the orbit ventrally to that of the *m. rectus ventralis* trigeminal nerve entrance. It inserts posteriorly around the eye.

**Innervation:** Abducens (VI) nerve (Edgeworth, 1935).

**M. rectus medialis** (Figure 9b; *m. rect. med.*)

**Description:** This has its origin relatively anteriorly to the other rectus muscles and is antagonistic to the *m. rectus lateralis*. It inserts anteriorly around the eye.

**Innervation:** Oculomotor (III) nerve (Edgeworth, 1935).

***M. obliquus ventralis*** (Figure 9b; *m. obl. vent.*)

**Description:** This is antagonistic to the *m. obliquus dorsalis*. It has its origin anterior to the foramen for the IV nerve. It inserts antero-ventrally around the eye.

**Innervation:** Oculomotor (III) nerve (Edgeworth, 1935).

***M. obliquus dorsalis*** (Figure 9b; *m. obl. dors.*)

**Description:** This is antagonistic to the *m. obliquus ventralis*. It has its origin just dorsal to that for the *m. obliquus ventralis*. It inserts antero-dorsally around the eye.

**Innervation:** Trochlear (IV) nerve (Edgeworth, 1935).

### 3.2.3 | Ligaments

**Ethmopalatine ligament** (Figure 8a; *lig. ethpal.*)

**Description:** This ligament links the palatoquadrate to the neurocranium. It attaches onto the posterior part of the nasal capsule and the anterior part of the suborbital shelf. It extends to attach on the anterior side of the ethmoid process of the palatoquadrate.

**Mandibulohyoid ligament** (not figured).

In elasmobranchs, a ligament binds the hyoid arch to the mandible (Wilga et al., 2000). However, contrast is insufficient to model this out in our scan data.

**Superior and inferior spiracular ligaments** (not figured).

In *Scyliorhinus*, two ligaments associated with the spiracle link the ceratohyal and hyomandibula to the neurocranium (Ridewood, 1896). However, the contrast around the spiracle is insufficient to model these in our data.

## 4 | DISCUSSION

The very different cranial constructions of *Callorhynchus* and *Scyliorhinus* are reflected in two very different arrangements of cranial muscles. In *Callorhynchus* and other holocephalans, muscles are arranged to accommodate an anteriorly placed mandible, extensive labial cartilages and a subcranial pharynx (Didier, 1995). In *Scyliorhinus* and other elasmobranchs, they are instead arranged around a hyostylic jaw suspension and elongated pharynx, with some variation within the group, particularly in the areas of the eyelid muscles and jaws (Soares & Carvalho, 2013). The evolution of these two divergent morphologies can be traced back to the origins of the two clades in the Palaeozoic, using the fossil record of stem-group and early crown-group Chondrichthyes, which preserve evidence of muscle morphology and attachments in the form of skeletal correlates and (very rarely) fossilized muscles. Assessing the relative evolution of these two types is somewhat hindered by the poorly understood

phylogenetic relationships of early members of the chondrichthyan crown and stem groups. Nonetheless, below we assess the relationships of muscles in the living taxa described above to those seen in their fossil relatives.

### 4.1 | The evolution of chondrichthyan jaw musculature

Chondrichthyan jaw suspensions, around which jaw muscles are arranged, show a wide array of anatomies (Maisey, 1980), all of which likely derive from a common form seen in Palaeozoic sharks. Variations in suspensory anatomy centre around the palatoquadrate's points of articulation with the neurocranium as well as the role of the hyoid arch in suspension. A prevalent idea among early vertebrate workers was that all gnathostome jaw suspensions derive from autodiastyly: an arrangement where the palatoquadrate is suspended from the neurocranium by otic and basal articulations and the hyomandibula is non-suspensory, and from which in theory all gnathostome jaw suspensions can be derived (De Beer & Moy-Thomas, 1935; Grogan & Lund, 2000; Grogan et al., 1999). Autodiastyly was originally hypothetical and does not exist in any living vertebrate, although comparisons have been drawn with holocephalan embryos (Grogan et al., 1999) and a comparable arrangement exists in the Palaeozoic stem-holocephalan *Debeerius* (Grogan & Lund, 2000). However, fossil morphologies in current phylogenetic topologies do not support the idea that this is the chondrichthyan ancestral state. Maisey (1980, 2001, 2008) argued that an autodiastylic chondrichthyan common ancestor was unlikely based on the prevalence of suspensory hyoid arches across the gnathostome crown group, as well as the suspensory hyoid arch and postorbital articulation of the palatoquadrate in *Pucapampella*, likely a stem-chondrichthyan. Since then this position has been strengthened as the chondrichthyan, stem group has been populated by several other taxa, including *Gladbachus*, *Doliodus* and *Acanthodes*, all of which possess a postorbital articulation and a suspensory hyoid arch (Brazeau & de Winter, 2015; Coates et al., 2018; Maisey et al., 2009). The identification of symmoriiiformes, which also have a hyomandibula articulating on the neurocranium and a postorbital articulation of the palatoquadrate, as stem-holocephalans further supports this (Coates et al., 2017), although the possibly reduced role of the hyoid arch in jaw suspension may be a precursor to the holocephalan state (Pradel et al., 2014). All this evidence points towards the holocephalan jaw suspension being derived from an ancestral state with ethmoid and postorbital articulation in what Maisey (2008) terms archaeostyly.

As a result of this, the divergent mandibular adductor musculature morphologies of holocephalans and elasmobranchs presumably derive from a more elasmobranch-like model. In *Callorhynchus* and other holocephalans, the mandibular adductors are located almost entirely preorbitally, directly linking the neurocranium and the lower jaw (Figure 3; Didier, 1995). In elasmobranchs, they instead lie post/suborbitally and attach to the mandibular cartilages

laterally. Anderson (2008) notes that the holocephalan condition has similarities with that of the osteichthyan *Amia*, with a neurocranial origin of the mandibular adductors and an insertion on tissue slung around the ventral side of the mandible. However, in chondrichthyans, this is certainly the more derived of the two conditions: stem-chondrichthyans such as *Acanthodes* and *Gladbachus*, as well as early crown-chondrichthyans such as *Tristychius* and *Akmonistion*, lack an anteriorly restricted mandible, and possess clear fossae for a mandibular adductor spanning the lateral sides of the mandibular cartilages as in elasmobranchs, and dorsally restricted by rims precluding attachment on the neurocranium (Coates et al., 2018, 2019; Coates & Sequeira, 2001; Miles, 1973). An Upper Devonian cladoselachian preserving palatoquadrates and parts of the mandibular adductor is also consistent with this morphology (Maisey, 1989). Based on the broad presence of this arrangement across chondrichthyan phylogeny, the holocephalan condition can only be interpreted as derived.

Labial muscles are present in both holocephalans and elasmobranchs, but the homologies between the two are uncertain. In holocephalans, the labial muscles are a suite of preorbital muscles inserting on the labial cartilages, the *mm. anguli oris* and the *m. labialis*, which together with the *m. intermandibularis* allow for manipulation of the upper and lower lips in feeding (Ribbink, 1971). In elasmobranchs, the labial muscles comprise the *m. levator labii superioris* (or *preorbitalis*), which links the palatoquadrate to the neurocranium anteriorly, and which varies in its attachment to the neurocranium in different groups (Wilga, 2005). Some living elasmobranchs also have well-developed labial cartilages (e.g. *Ginglymostoma*, Motta et al., 2008); however, unlike those of holocephalans, these have poorly developed muscle attachments (Maisey, 1983), and instead laterally occlude the mouth during suction feeding creating a more effective oral aperture. Anderson (2008) argued that labial muscles in elasmobranchs and holocephalans are homologous on the basis that they are both preorbital facial muscles with a trigeminal (V) innervation that insert, at least in part, on the mandible (although we found no evidence for such an insertion in *Callorhynchus*). Unfortunately, corroborating evidence in stem-group and early crown-group chondrichthyans is limited. Although a labial muscle has been reconstructed in *Acanthodes* and *Cladodus* (Lauder, 1980), this is not on the basis of any positive fossil evidence—the muscle leaves no clear skeletal attachment areas, and is not observable in cladoselachian specimens preserving muscles (Maisey, 1989, 2007). Several stem-group elasmobranchs (e.g. *Egertonodus*, *Tristychius*) have numerous, smaller labial cartilages ostensibly more like those of living holocephalans than elasmobranchs (Maisey, 1983). However, in at least *Tristychius*, these have been shown to play a role similar to that of suction feeding extant elasmobranchs (Coates et al., 2019). If elasmobranch and holocephalan labial cartilages are homologous, the shift to a holocephalan-like insertion on the labial cartilages is presumably linked to the evolution of extensive labial cartilages, holostyly and crown-holocephalan-like feeding, and so would likely have taken place at some point in the stem group after the divergence of symmoriiforms. However, it remains difficult to see a clear skeletal correlate.

However, the morphology of fossil holocephalan neurocrania does provide some clues and constraints on when their preorbital mandibular muscle morphology arose. Mesozoic stem-group holocephalans—*Acanthorhina*, *Chimaeropsis*, *Metopacanthus*, *Squaloraja* and *Isychodus*—are reconstructed with skulls with a large rostrum, shaped in such a way as to allow attachment of preorbital mandibular musculature, although their flattened skulls make this difficult to know definitively (Patterson, 1965). Moreover, the Palaeozoic holocephalan *Chondrenchelys* is interpreted as having had adductor muscles that attached preorbitally on the basis of the morphology of its preorbital region (Finarelli & Coates, 2014). As Finarelli and Coates (2014) highlight, an anteriorly restricted mandible and ventral gill skeleton are not present in *Chondrenchelys*, which could suggest that the preorbital attachment of mandibular adductors preceded these shifts (although see the discussion of likely homoplasy in stem-holocephalans below). *Debeerius* also possesses a large rostral region, although Grogan and Lund (2000) interpret the adductor muscles as having attached on the posterior part of the palatoquadrate. Providing a lower boundary on the morphology are the more shark-like stem-holocephalans such as symmoriiformes, which have neurocrania and jaws incompatible with a crown-holocephalan-like configuration (see above). Several edestids have enlarged rostra (most obviously *Ornithoprion*; Zangerl, 1966), but also separate palatoquadrates with posteriorly located adductor muscles (see *Helicoprion*; Ramsay et al., 2015). This suggests that the development of a large ethmoid region in the holocephalan stem group preceded the fusion of the palatoquadrates with the neurocranium and the shift of the adductor muscles onto the neurocranium, which took place somewhere between the divergence of edestids and *Chondrenchelys* from the crown lineage.

A curious exception that does not fit this pattern is iniopterygians, another member of the holocephalan stem group. Like in living holocephalans, this group possesses anteriorly placed Meckel's cartilages with a medial symphysis, palatoquadrates fused to the neurocranium (in some members) and a subcranial branchial skeleton (Pradel, 2010; Pradel et al., 2009). As three-dimensional specimens of "*Iniopera*" show, the large orbits would have obstructed a postorbital attachment of the adductor muscles (Pradel, 2010; Pradel et al., 2009). However, a large rostral surface for a preorbital attachment of the adductor muscles is decidedly absent. Instead, a very shallow fossa above the quadrate articulation in the suborbital shelf provides a possible attachment points (Pradel, 2010; Figures 6 and 11), as does the small preorbital surface (Pradel, 2010; Figure 6). If two mandibular adductors were present, as in *Callorhynchus*, it is possible that the fossa in the orbit provided attachment for the posterior mandibular adductor while the anterior mandibular adductor attached preorbitally. Notably, "*Iniopera*" also possesses ventrally delimited fossae on the postero-lateral sides of the Meckel's cartilages, possibly to house the ventral adductor (Pradel, 2010; figure 31, fam), suggesting the muscles were not slung ventrally around the jaw as in living holocephalans. Which of this set of traits is homologous with those

of crown-holocephalans or homoplasies linked to iniopterygians derived form is unclear. However, iniopterygians do demonstrate that once holostyly and anteriorly placed adductor muscles had evolved, a large-rostrumed holocephalan-like form was not an inevitability.

As well as the facial muscles, the large coracomandibularis is an unusual feature of the holocephalan mandibular musculature. In both holocephalans and elasmobranchs, the lower jaw is depressed by the coracomandibularis muscle, unlike in osteichthyans which use the coracohyoideus to transmit movement through the mandibulo-hyoid ligament (Anderson, 2008). A chondrichthyan-like arrangement was also present in mandibulate stem-gnathostomes, and so is likely the ancestral state for crown-group gnathostomes (Johanson, 2003). However, within chondrichthyans, the coracomandibularis of holocephalans (e.g. *Callorhinchus*, Figure 4) is far larger than that of *Scyliorhinus* and other chondrichthyans and attaches over a greater area both on the shoulder girdle and on the mandible. Again, evidence for the presence of this muscle is limited in the holocephalan stem group, but it seems likely to be part of the suite of adaptations linked to durophagy and a ventrally located pharynx. In the stem-holocephalan *Iniopera*, the shoulder girdle and mandible have an extremely close association (Pradel pers. obs.) possibly placing the evolution of a large, short coracomandibularis as far back in the holocephalan stem group as crown-holocephalans' divergence from iniopterygians.

## 4.2 | Pharyngeal muscles

The non-suspensory nature of the holocephalans hyoid arch as well as its supposed "morphologically-complete" nature has been used to argue that they represent the primitive gnathostome condition (Grogan & Lund, 2000), but both are likely derived. Maisey (1984) outlined why the holocephalan condition is unlikely to be plesiomorphic for chondrichthyans on the basis of a convincing set of anatomical arguments. This included the fact that the holocephalan hyoid arch is bypassed by the branchial muscles linking the dorsal branchial series, the condition seen in *Callorhinchus*. In stem-chondrichthyans such as *Glabdachus* and *Acanthodes*, the hyomandibula articulates directly with the neurocranium and lacks a pharyngohyal (Brazeau & de Winter, 2015; Coates et al., 2018), and the same state is seen in shark-like putative stem-holocephalans (e.g. *Ozarcus*; Pradel et al., 2014) strongly suggesting that this condition is plesiomorphic for the chondrichthyan crown group. This implies that hypotheses based on the idea that the holocephalan branchial skeleton and jaw articulation are primitive are incorrect, and it seems likely that a more elasmobranch-like arrangement is primitive for chondrichthyans. If autapomorphic the holocephalan pharyngohyal is perhaps instead linked to the holocephalan hyoid arch's role in supporting the roof of the pharynx, or with the role it plays in supporting the operculum. The ligament we report linking the pharyngohyal to the basicranium may anchor the hyoid arch to the neurocranium for one (or both) of these purposes.

Although both holocephalans and elasmobranchs possess a *coracomandibularis*, linking mandible and shoulder girdle, holocephalans alone possess a *mandibulo-hyoideus* (*inter-hyoideus* of Didier (1995), *genio-hyoideus* of Kesteven (1933)) linking the mandible to the ceratohyal. Although morphologically similar to the *genio-hyoideus* of osteichthyans, Anderson (2008) argues that the muscles are not homologous. Rather, the plesiomorphic means of depressing the mandible in crown-gnathostomes is broadly thought to be achieved by the coracomandibularis (Anderson, 2008; Johanson, 2003, p. 20; Wilga et al., 2000). In living holocephalans like *Callorhinchus*, the muscle attaches to a pronounced ventral process on the broad ceratohyal. *Iniopera* also possesses a large, flat ceratohyal with a similar process, suggesting that this morphology was present at least in iniopterygians in the holocephalan stem group (Pradel pers. obs.). *Ozarcus*, as well as stem-chondrichthyans such as *Acanthodes*, *Ptomacanthus* and *Glabdachus* instead have long, thin ceratohyals with no such process (Coates et al., 2018; Dearden et al., 2019; Miles, 1973; Pradel et al., 2014) bolstering the idea that such a muscle was absent in the early holocephalan and chondrichthyan stem groups, and that its evolution is linked to a holostylic jaw suspension. However, it is difficult to rule out the possibility completely: in osteichthyans with a *genio-hyoideus*, for example, *Amia* (Allis, 1897; Anderson, 2008), the ceratohyal is not necessarily long and thin. If this muscle is novel in chimaeroids, it may be linked to their unusual ventilatory process, which is based on fore-aft movements (Dean et al., 2012) and which may have been present in some chondrichthyan stem-group members (Pradel pers. obs.).

The extended and compact pharynxes in elasmobranchs and holocephalans, respectively, necessitate major differences in branchial musculature. Although a subcranial pharynx is likely plesiomorphic for crown-group gnathostomes and is present in some stem-chondrichthyans (Dearden et al., 2019), it does seem that a posteriorly extended pharynx was present at the divergence of elasmobranchs and holocephalans, given this state in several stem-chondrichthyans and putative stem-holocephalans (Coates et al., 2018; Pradel et al., 2014). Despite the major shift to a holocephalan condition, many of the muscles of the elasmobranch pharynx are preserved in *Callorhinchus* including hyoid and branchial constrictors, the *subspinalis* muscle, *interpharyngobranchialis* muscles and the *interarcuales* muscles, suggesting that these were present in the ancestral crown-chondrichthyan. Linked to this shift is the close muscular association of the neurocranium with the scapulocoracoid via the *cucullaris superficialis*, *cucullaris profundus* and *protractor dorsalis pectoralis*. Skeletal correlates for these muscles are difficult to find, but a subcranial branchial skeleton is present in several Palaeozoic stem-holocephalans including iniopterygians and *Debeerius*, suggesting that they may have been present (Grogan & Lund, 2000; Pradel et al., 2010). In *Chondrenchelys*, the branchial skeleton appears to be more posteriorly placed (Finarelli & Coates, 2014). Given this and the extended pharynxes of some stem-chondrichthyans and stem-holocephalans, an elasmobranch-like extended cucullaris seems likely to be plesiomorphic for chondrichthyans, with separate *cucullaris profundus* and *cucullaris superficialis* muscles having evolved in the holocephalan stem-group perhaps crownwards relative to *Chondrenchelys*.

A holocephalan-like hyoid operculum with its greatly enlarged hyoid constrictor muscles seems likely to be derived and linked to a ventrally placed branchial skeleton. However, its presence/absence can be difficult to detect in the fossil record as the evidence for gill slits/operculae is often indirect. In one Upper Devonian cladoselachian specimen, the muscles and branchial rays are preserved, demonstrating an elasmobranch-like arrangement of both (Maisey, 1989). In several other Palaeozoic “sharks”, posteriorly extended branchial skeletons such as *Triodus* and *Tristychius* operculae have been inferred on the basis of enlarged hyoid rays, although some of these have since been disputed (discussed in Coates et al., 2018, supp. mat.). An enlarged hyoid operculum is not necessarily mutually exclusive with posteriorly extending branchial arches. In several acanthodian-grade stem-chondrichthyans, where the gill slits are observable in the patterning of the dermal shagreen, both an enlarged hyoid operculum and several posterior gill slits can be observed (Watson, 1937). So, while the holocephalan sub-neurocranial pharynx is derived, an enlarged operculum may run deeper into the holocephalan, or even chondrichthyan, stem-group.

#### 4.3 | Crown-chondrichthyan phylogeny and cranial muscles

Our observations on muscle morphology in living and fossil chondrichthyans fit into a shifting understanding of crown-group chondrichthyan relationships. A growing body of evidence suggests that numerous early Palaeozoic “sharks” are early crown-group chondrichthyans, placing symmoriiformes and *Cladoselache* in the holocephalan stem group, and ctenacanths, xenacanths and *Cladodoides* in the elasmobranch stem group (Coates et al., 2017; Frey et al., 2019). Our evidence on the muscles of *Callorhinchus*, suggesting modern holocephalan cranial muscles originated in an elasmobranch-like form, is consistent with this (although also with opposing arguments that these taxa are stem-chondrichthyans, see Pradel et al. (2011)). Within holocephalans, recent phylogenetic analyses place iniopterygians as the sister group to the crown group, *Helodus*, *Chondrenchelys* and *Debeerius* (e.g. Coates et al., 2017; Frey et al., 2019), perhaps suggesting that preorbital mandibular adductors unites these taxa with iniopterygians, and the movement of the adductors onto a broad ethmoid surface groups them to the exclusion of iniopterygians. However, not all character distributions are clear cut in this phylogenetic topology; in the eel-like *Chondrenchelys*, the branchial region is extended (Finarelli & Coates, 2014), unlike the subcranial pharynx of crown-holocephalans and the less crownward-placed iniopterygians and *Debeerius* (Grogan & Lund, 2000; Zangerl and Case, 1973). Also notably, these analyses do not incorporate presumed stem-holocephalan taxa such as caseodonts and eugeneodontids, which combine a shark-like form with enlarged preorbital regions (Zangerl, 1981). Confusing matters even further is the variability in morphologies even within presumed stem-holocephalan clades, with Iniopterygia

and Eugeneodontida (both *sensu* Zangerl, 1981) including a mixture of taxa with palatoquadrates fused (e.g. “*Iniopera*”, *Ornithoprion*; Pradel, 2010, Zangerl, 1966) and not fused (e.g. *Iniopteryx*, *Helicoprion*; Zangerl, 1981, Tapanila et al., 2013) to the neurocranium. More fine-grained understanding of holocephalan phylogeny seems likely to reveal considerable homoplasy, rather than an inexorable evolutionary march towards a chimaeroid-like head.

## 5 | CONCLUSIONS

Here, for the first time, we completely describe cranial muscle arrangements in a model holocephalan and elasmobranch using 3D digital methods. The reduced, but recognizably shark-like branchial musculature we identify in *Callorhinchus*, and the likely derived origins of most holocephalan cranial musculature based on fossil evidence, fit into an emerging picture where holocephalan anatomy comprises a set of apomorphic conditions with their origins in a shark-like form (Coates et al., 2018). Parts of this holocephalan anatomical suite, such as the unique hyoid arch morphology and *mandibulohyoideus*, may be functionally linked to their novel mode of respiration (Dean et al., 2012). A shark-like cranial musculature, with an extended pharynx and a postorbital and ethmoid jaw suspension, seems the likely ancestral state at the chondrichthyan crown-node. Digital dissections provide a unique way of describing and sharing anatomical structures in 3D and can help identify muscles which are difficult to view in gross dissection. However, this should be seen as a complement, rather than a substitute, to traditional methods as the resolution of scan data and the inability to manipulate and examine tissues directly create limitations on what can be seen. We hope these data will, alongside digital dissections from a broad array of organisms, help others to make better inferences on the origin and evolution of the vertebrate head.

## ACKNOWLEDGEMENTS

We thank the ID-19 beamline at the European Synchrotron Radiation Facility for assistance with scanning. Assistance in getting fresh *Scyliorhinus canicula* specimens from Didier Casane and Véronique Borday-Birraux from the Laboratoire Evolution Génomes Comportement Ecologie—CNRS, and Patrick Laurenti (Laboratoire Interdisciplinaire des Energies de Demain; Université Paris-Diderot) is gratefully acknowledged. We thank Florent Goussard (CR2P-MNH) for his inestimable help in 3D work. Some of this work began at the AMNH with the help of John Maisey.

## AUTHOR CONTRIBUTIONS

RPD, AH and AP conceived and designed the study. PT and AP scanned the specimens. RPD, RM, AC and AP processed the scan data. RPD analysed the data, with input from AP, AH and DD. RPD wrote the paper and made figures. All authors read and provided feedback on the manuscript.

## DATA AVAILABILITY STATEMENT

All 3D models are freely available via morphoMuseum (Dearden et al., 2021). Tomographic data are available on request from the authors.

## ORCID

Richard P. Dearden  <https://orcid.org/0000-0003-3522-7304>

Rohan Mansuit  <https://orcid.org/0000-0002-4727-3650>

Anthony Herrel  <https://orcid.org/0000-0003-0991-4434>

Paul Tafforeau  <https://orcid.org/0000-0002-5962-1683>

## REFERENCES

- Allis, E.P. (1897) The cranial muscles of *Amia*. *Journal of Morphology*, XII, 489–772.
- Allis, E.P. (1917) The homologies of the muscles related to the visceral arches of the gnathostome fishes. *Quarterly Journal of Microscopical Science*, 62, 303–406.
- Anderson, P.S.L. (2008) Cranial muscle homology across modern gnathostomes. *Biological Journal of the Linnean Society*, 94, 195–216.
- Brazeau, M.D. & de Winter, V. (2015) The hyoid arch and braincase anatomy of *Acanthodes* support chondrichthyan affinity of 'acanthodians'. *Proceedings of the Royal Society B: Biological Sciences*, 282, 20152210.
- Brocklehurst, R., Porro, L., Herrel, A., Adriaens, D. & Rayfield, E.J. (2019) A digital dissection of two teleost fishes: comparative functional anatomy of the cranial musculoskeletal system in pike (*Esox lucius*) and eel (*Anguilla anguilla*). *Journal of Anatomy*, 235, 189–204.
- Camp, A.L., Scott, B.R., Brainerd, E.L. & Wilga, C.D. (2017) Dual function of the pectoral girdle for feeding and locomotion in white-spotted bamboo sharks. *Proceedings of the Royal Society B: Biological Sciences*, 284(1859), 20170847.
- Coates, M.I., Finarelli, J.A., Sansom, I.J., Andreev, P.S., Criswell, K.E., Tietjen, K. et al. (2018) An early chondrichthyan and the evolutionary assembly of a shark body plan. *Proceedings of the Royal Society B: Biological Sciences*, 285(1870), 20172418.
- Coates, M.I., Gess, R.W., Finarelli, J.A., Criswell, K.E. & Tietjen, K. (2017) A symmoriiform chondrichthyan braincase and the origin of chimaeroid fishes. *Nature*, 541(7636), 208–211.
- Coates, M.I. & Sequeira, S.E.K. (2001) A new stethacanthid chondrichthyan from the lower Carboniferous of Bearsden, Scotland. *Journal of Vertebrate Paleontology*, 21, 438–459.
- Coates, M.I., Tietjen, K., Olsen, A.M. & Finarelli, J.A. (2019) High-performance suction feeding in an early elasmobranch. *Science Advances*, 5(9), eaax2742.
- Coolen, M., Menuet, A., Chassoux, D., Compagnucci, C., Henry, S., Leveque, L. et al. (2008) The dogfish *Scyliorhinus canicula*: a reference in jawed vertebrates. *Cold Spring Harbor Protocols*, 2008(12), pdb.em011.
- Cox, P.G. & Faulkes, C.G. (2014) Digital dissection of the masticatory muscles of the naked mole-rat, *Heterocephalus glaber* (Mammalia, Rodentia). *PeerJ*, 2014, 1–19.
- de Beer, G.R. (1931) The development of the skull of *Scyllium* (*Scyliorhinus*) *canicula* L. *Quarterly Journal of Microscopical Science*, 74, 591–652.
- De Beer, G.R. & Moy-Thomas, J.A. (1935) On the skull of Holocephali. *Philosophical Transactions of the Royal Society of London. Series B, Biological sciences*, 224, 287–312.
- Dean, M.N., Summers, A.P. & Ferry, L.A. (2012) Very low pressures drive ventilatory flow in chimaeroid fishes. *Journal of Morphology*, 273, 461–479.
- Dearden, R.P., Mansuit, R., Cuckovic, A. et al. (2021) 3D models related to the publication: The morphology and evolution of chondrichthyan cranial muscles: a digital dissection of the elephantfish *Callorhynchus milii* and the catshark *Scyliorhinus canicula*. *MorphoMuseuM*, 6, e133. <https://doi.org/10.18563/journam.3.133>
- Dearden, R.P., Stockey, C. & Brazeau, M.D. (2019) The pharynx of the stem-chondrichthyan *Ptomacanthus* and the early evolution of the gnathostome gill skeleton. *Nature Communications*, 10, 1–7.
- Denton, J.S.S., Maisey, J.G., Grace, M., Pradel, A., Dosey, M.H., Bart Jr., H.L. et al. (2018) Cranial morphology in *Mollisquama* sp. (Squaliformes; Dalatiidae) and patterns of cranial evolution in dalatiid sharks. *Journal of Anatomy*, 233, 15–32.
- Didier, D.A. (1995) Phylogenetic systematics of extant chimaeroid fishes (Holocephali, Chimaeroidei). *American Museum Novitates*, 3119, 1–86.
- Didier, D.A., Leclair, E.E. & Vanbuskirk, D.R. (1998) Embryonic staging and external features of development of the chimaeroid fish, *Callorhynchus milii* (Holocephali, Callorhynchidae). *Journal of Morphology*, 47, 25–47.
- Edgeworth, F.H. (1902) The development of the head muscles in *Scyllium canicula*. *Journal of Anatomy and Physiology*, 37, 73–88.
- Edgeworth, F.H. (1935) *The Cranial Muscles of Vertebrates*. London, UK: Cambridge University Press.
- Frey, L., Coates, M., Ginter, M., Hairapetian, V., Rücklin, M., Jerjen, I., et al. (2019) The early elasmobranch *Phoebodus*: phylogenetic relationships, ecomorphology and a new time-scale for shark evolution. *Proceedings of the Royal Society B*, 28620191336.
- Finarelli, J.A. & Coates, M.I. (2014) *Chondrenchelys problematica* (Traquair, 1888) redescribed: a Lower Carboniferous, eel-like holocephalan from Scotland. *Earth and Environmental Science Transactions of The Royal Society of Edinburgh*, 105, 35–59.
- Gilbert, S.G. (1965) *Pictorial Anatomy of the Dogfish*. Seattle: University of Washington Press.
- Grogan, E.D. & Lund, R. (2000) *Debeerius ellefseni* (Fam. Nov., Gen. Nov., Spec. Nov.), an autodiastylid chondrichthyan from the Mississippian Bear Gulch Limestone of Montana (USA), the relationships of the chondrichthyes, and comments on gnathostome evolution. *Journal of Morphology*, 245, 219–245.
- Grogan, E.D., Lund, R. & Didier, D.A. (1999) Description of the chimaerid jaw and its phylogenetic origins. *Journal of Morphology*, 59, 45–59.
- Holmgren, N. (1940) Development of the skull in sharks and rays. *Acta Zoologica*, 21, 51–216.
- Hughes, G.M. & Ballintijn, C.M. (1965) The muscular basis of the respiratory pumps in the dogfish (*Scyliorhinus canicula*). *Journal of Experimental Biology*, 43, 363–383.
- Inoue, J.G., Miya, M., Lam, K., Tay, B.-H., Danks, J.A., Bell, J. et al. (2010) Evolutionary origin and phylogeny of the modern holocephalans (Chondrichthyes: Chimaeriformes): a mitogenomic perspective. *Molecular Biology and Evolution*, 27, 2576–2586.
- Johanson, Z. (2003) Placoderm branchial and hypobranchial muscles and origins in jawed vertebrates. *Journal of Vertebrate Paleontology*, 23, 735–749.
- Kesteven, H.L. (1933) The anatomy of the head in *Callorhynchus antarcticus*. *Journal of Anatomy*, 67, 443–474.
- Klinkhamer, A.J., Wilhite, D.R., White, M.A. & Wroe, S. (2017) Digital dissection and three-dimensional interactive models of limb musculature in the Australian estuarine crocodile (*Crocodylus porosus*). *PLoS ONE*, 12, 17–22.
- Lauder, G.V. (1980) On the evolution of the jaw adductor musculature in primitive gnathostome fishes. *Breviora*, 460, 1–10.
- Lautenschlager, S., Bright, J.A. & Rayfield, E.J. (2014) Digital dissection – using contrast-enhanced computed tomography scanning to elucidate hard- and soft-tissue anatomy in the Common Buzzard, *Buteo buteo*. *Journal of Anatomy*, 224, 412–431.
- Licht, M., Schmuecker, K., Huelsken, T., Hanel, R., Bartsch, P. & Paeckert, M. (2012) Contribution to the molecular phylogenetic analysis of extant holocephalan fishes (holocephali, chimaeriformes). *Organisms, Diversity, & Evolution*, 12, 421–432.
- Luther, A.F. (1909a) Beiträge zur Kenntnise von Muskulatur und Skelett des Kopfes des Haies *Stegostoma tigrinum* Gm. und der Holocephalen

- mit einem Anhang ueber die. *Acta Societas Scientiarum Fennicae*, 37, 1–50.
- Luther, A.F. (1909b) Untersuchungen ueber die von *N. trigeminus* innervierte Musculatur der Selachier (Haie und Rochen) unter Beruecksichtigung ihrer Beziehungen zu benachbarten Organen. *Acta Societas Scientiarum Fennicae*, 36, 1–176.
- Maisey, J.G. (1980) An evaluation of jaw suspension in sharks. *American Museum Novitates*, 2706, 1–17.
- Maisey, J.G. (1983) Cranial anatomy of *Hybodus basanus* Egerton from the Lower Cretaceous of England. *American Museum Novitates*, 2758, 1–64.
- Maisey, J.G. (1984) Chondrichthyan phylogeny: a look at the evidence. *Journal of Vertebrate Paleontology*, 4, 359–371.
- Maisey, J.G. (1989) Visceral skeleton and musculature of a Late Devonian shark. *Journal of Vertebrate Paleontology*, 9, 174–190.
- Maisey, J.G. (2001) A primitive chondrichthyan braincase from the Middle Devonian of Bolivia. In: Ahlberg, P.E. (Ed.) *Major Events in Early Vertebrate Evolution*. London, UK: Taylor and Francis, pp. 263–288.
- Maisey, J.G. (2007) The braincase in palaeozoic symmoriform and cladoselachian sharks. *Bulletin of the American Museum of Natural History*, 307, 1–122.
- Maisey, J.G. (2008) The postorbital palatoquadrate articulation in elasmobranchs. *Journal of Morphology*, 269, 1022–1040.
- Maisey, J.G., Miller, R.F. & Turner, S. (2009) The braincase of the chondrichthyan *Doliodus* from the Lower Devonian Campbellton Formation of New Brunswick, Canada. *Acta Zoologica*, 90, 109–122. <https://doi.org/10.1111/j.1463-6395.2008.00330.x>
- Marinelli, W. & Strenger, A. (1959) *Vergleichende anatomie und morphologie der wirbeltiere. III. Lieferung. Squalus acanthias*. Wien: Deiticke, 173–308.
- Miles, R.S. (1973) Relationships of acanthodians. In: Greenwood, P., Miles, R.S. & Patterson, C. (Eds.) *Interrelationships of Fishes*. London: Zoological Journal of the Linnean Society, pp. 63–103.
- Motta, P.J. & Huber, D.R. (2012) Prey capture behavior and feeding mechanisms of elasmobranchs. In: Musick, J., Carrier, J. & Heithaus, M. (Eds.) *Biology of sharks and their relatives*. Boca Raton: CRC Press, pp. 153–209.
- Motta, P.J., Hueter, R.E., Tricas, T.C., Summers, A.P., Huber, D.R. & Lowry, D. (2008) Functional morphology of the feeding apparatus, feeding constraints, and suction performance in the nurse shark *Ginglymostoma cirratum*. *Journal of Morphology*, 268, 1041–1055.
- Nakaya, K. (1975) Taxonomy, comparative anatomy, and phylogeny of Japanese catsharks, Scyliorhinidae. *Memoirs of the Faculty of Fisheries, Hokkaido University*, 23, 1–94.
- Nelson, J.S., Grande, T.C. & Wilson, M.V.H. (2016) *Fishes of the World*. Hoboken: Wiley.
- Oulion, S., Borday-Birraux, V., Debais-Thibaud, M., Mazan, S., Laurenti, P. & Casane, D. (2011) Evolution of repeated structures along the body axis of jawed vertebrates, insights from the *Scyliorhinus canicula* Hox code: evolution of repeated structures, insights from the *S. canicula* Hox code. *Evolution & Development*, 13, 247–259.
- Parker, W.K. (1878) The structure and development of the skull in sharks and skates. *Transactions of the Zoological Society*, 10(4), 189–234.
- Patterson, C. (1965) The phylogeny of the chimaeroids. *Philosophical Transactions of the Royal Society of London. Series B, Biological Sciences*, 249, 101–219.
- Porro, L.B. & Richards, C.T. (2017) Digital dissection of the model organism *Xenopus laevis* using contrast-enhanced computed tomography. *Journal of Anatomy*, 231, 169–191.
- Pradel, A. (2010) Skull and brain anatomy of Late Carboniferous Sibirhynchidae Skull and brain anatomy of Late Carboniferous Sibirhynchidae (Chondrichthyes, Iniopterygia) from Kansas and Oklahoma (USA). *Geodiversitas*, 32, 595–661.
- Pradel, A., Didier, D.A., Casane, D., Tafforeau, P. & Maisey, J.G. (2013) Holocephalan embryo provides new information on the evolution of the glossopharyngeal nerve, metotic fissure and parachordal plate in gnathostomes. *PLoS ONE*, 8, e66988.
- Pradel, A., Langer, M., Maisey, J.G., Geffard-Kuriyama, D., Cloetens, P., Janvier, P. et al. (2009) Skull and brain of a 300-million-year-old chimaeroid fish revealed by synchrotron holotomography. *Proceedings of the National Academy of Sciences of the United States of America*, 106, 5224–5228.
- Pradel, A., Maisey, J.G., Tafforeau, P., Mapes, R.H. & Mallatt, J. (2014) A Palaeozoic shark with osteichthyan-like branchial arches. *Nature*, 509, 608–611.
- Pradel, A., Tafforeau, P. & Janvier, P. (2010) Study of the pectoral girdle and fins of the Late Carboniferous sibirhynchid iniopterygians (Vertebrata, Chondrichthyes, Iniopterygia) from Kansas and Oklahoma (USA) by means of microtomography, with comments on iniopterygian relationships. *Comptes Rendus Palevol*, 9, 377–387.
- Pradel, A., Tafforeau, P., Maisey, J.G. & Janvier, P. (2011) A new paleozoic symmoriformes (chondrichthyes) from the late carboniferous of Kansas (USA) and cladistic analysis of early chondrichthyans. *PLoS ONE*, 6(9), e24938.
- Raikow, R.J. & Swierczewski, E.V. (1975) Functional anatomy and sexual dimorphism of the cephalic clasper in the pacific ratfish (*Chimaera collei*). *Journal of Morphology*, 145, 435–439. <https://doi.org/10.1002/jmor.1051450404>
- Ramsay, J.B., Wilga, C.D., Tapanila, L., Pruitt, J., Pradel, A., Schlader, R. et al. (2015) Eating with a saw for a jaw: functional morphology of the jaws and tooth-whorl in *Helicoprion davisii*. *Journal of Morphology*, 276, 47–64.
- Reif, W.E. (1980) Development of dentition and dermal skeleton in embryonic *Scyliorhinus canicula*. *Journal of Morphology*, 166(3), 275–288.
- Ribbink, A.J. (1971) Contributions to the functional morphology of fishes part VI: the jaw mechanism and feeding of the holocephalan, *Callorhynchus capensis* Dumeril. *Zoologica Africana*, 6(1), 45–73.
- Ridewood, W.G. (1896) On the spiracle and associated structures in elasmobranch fishes. *Anatomischer Anzeiger*, 11, 425–433.
- Ridewood, W.G. (1899) On the eyelid-muscles of the carchariidae and *Scyllium*: a contribution to the morphology of the nictitating membrane of sharks. *Journal of Anatomy and Physiology*, 33, 228–242.
- Shann, E.W. (1919) The comparative myology of the shoulder girdle and pectoral fin of fishes. *Transactions of the Royal Society of Edinburgh*, 52, 531–570.
- Sharp, A.C. & Trusler, P.W. (2015) Morphology of the jaw-closing musculature in the common wombat (*Vombatus ursinus*) using digital dissection and magnetic resonance imaging. *PLoS ONE*, 10, 1–19.
- Soares, M.C. & Carvalho, M.R.D. (2013) Mandibular and Hyoid Muscles of Galeomorph Sharks (Chondrichthyes: Elasmobranchii), with remarks on their phylogenetic intrarelationships. *Journal of Morphology*, 274, 203–214. <https://doi.org/10.1002/jmor.20166>
- Tapanila, L., Pruitt, J., Pradel, A., Wilga, C.D., Ramsay, J.B., Schlader, R. et al. (2013) Jaws for a spiral-tooth whorl: CT images reveal novel adaptation and phylogeny in fossil *Helicoprion*. *Biology Letters*, 9, 20130057.
- Tomita, T., Toda, M., Miyamoto, K., Ueda, K. & Nakaya, K. (2018) Morphology of a hidden tube: resin injection and CT scanning reveal the three-dimensional structure of the spiracle in the Japanese Bullhead Shark *Heterodontus japonicus* (Chondrichthyes; Heterodontiformes; Heterodontidae). *Anatomical Record*, 301, 1336–1341.
- Vetter, B. (1878) Untersuchungen zur vergleichenden Anatomie der Kiemen- und Kiefermuskeln der Fische. II Teil. *Jena Z Naturwiss*, 12, 431–550.
- Watson, D.M.S. (1937) The Acanthodian fishes. *Philosophical Transactions of the Royal Society of London. Series B, Biological sciences*, 228, 49–146.

- Wilga, C.D. (2005) Morphology and evolution of the jaw suspension in lamniform sharks. *Journal of Morphology*, 265, 102–119.
- Wilga, C.D., Wainwright, P.C. & Motta, P.J. (2000) Evolution of jaw depression mechanics in aquatic vertebrates: insights from chondrichthyes. *Biological Journal of the Linnean Society*, 71, 165–185.
- Zangerl, R. (1966) A new shark of the family Edestidae, *Ornithoprion herwigii*, from the Pennsylvanian Mecca and Logan quarry shales of Indiana. *Fieldiana*, 16, 1–43.
- Zangerl, R. & Case, G.R. (1973) Iniopterygia, a new order of chondrichthyan fishes from the Pennsylvanian of North America. *Fieldiana Geology*, 6, 1–67.
- Zangerl, R. (1981) *Handbook of Paleichthyology, Chondrichthyes I, Paleozoic Elasmobranchii*. Schultze, H.P. (Ed.). Stuttgart: Gustav Fischer Verlag, 115 pp.
- Ziermann, J.M., Miyashita, T. & Diogo, R. (2014) Cephalic muscles of Cyclostomes (hagfishes and lampreys) and Chondrichthyes (sharks, rays and holocephalans): comparative anatomy and early evolution

of the vertebrate head muscles. *Zoological Journal of the Linnean Society*, 172, 771–802.

#### SUPPORTING INFORMATION

Additional supporting information may be found online in the Supporting Information section.

**How to cite this article:** Dearden RP, Mansuit R, Cuckovic A, et al. The morphology and evolution of chondrichthyan cranial muscles: A digital dissection of the elephantfish *Callorhynchus milii* and the catshark *Scyliorhinus canicula*. *J Anat.* 2021;238:1082–1105. <https://doi.org/10.1111/joa.13362>